Two Systems, Two Timelines: Computational Evidence for Dissociable Development in Inhibitory Control Across Childhood and Adolescence

Abstract

This study examined inhibitory control development in two samples of Chinese children: a primary sample (n = 1,122; 45.5% female; 91.9% Han, M_{age} = 12.42 years, range: 6.0–18.7) with 6-month longitudinal follow-up and an independent replication sample (n = 1,026; 45.1% female; 90.8% Han, M_{age} = 12.44 years, range: 6.1–18.8). Generalized Additive Models applied to *Stroop* and *Go/No-Go* tasks revealed four-phase nonlinear developmental trajectories. Response inhibition stabilized by 13.4 years, while interference inhibition developed until 15.8 years. Hierarchical drift diffusion modeling showed that interference inhibition developed through enhanced information accumulation (drift rate), whereas response inhibition developed through enhanced response bias control (starting point). Age-related processing speed improvements suggest shared foundational mechanisms. The findings contribute to a decision-computational framework.

Keywords: inhibitory control; nonlinear development; drift diffusion model; generalized additive model; machine learning

Introduction

When a child struggles to complete homework while siblings play nearby, or when a teenager impulsively responds to a text message during class, we witness the real-world consequences of developing inhibitory control. Inhibitory control—a core executive function

enabling the suppression of inappropriate responses in favor of goal-directed behavior—develops gradually from early childhood through adolescence (Diamond, 2013). This capacity predicts numerous positive developmental outcomes, including enhanced social competence (Beauchamp & Anderson, 2010), reduced internalizing problems (Nigg, 2017), and improved academic achievement (Allan et al., 2014). Conversely, deficits in inhibitory control are associated with persistent attention problems, emotion dysregulation, and impulse control challenges (Nigg et al., 2017). Despite decades of research, however, fundamental questions about the development of this critical ability remain unanswered. Consider a concrete example: when children watch educational videos with distracting advertisements, some can filter out these irrelevant stimuli while maintaining focus, whereas others struggle to suppress immediate reactions to the colorful animations. These contrasting patterns exemplify two distinct forms of inhibitory control that emerge throughout childhood: interference inhibition and response inhibition. Such observations raise a fundamental question: if inhibitory control develops as a unified capacity, why do older children not consistently outperform younger ones across both forms? These developmental patterns reveal substantial complexity, suggesting that these abilities may follow independent trajectories and rely on distinct computational

The Multi-Component Nature of Inhibitory Control and its Developmental Patterns

Research has identified two primary components of inhibitory control: interference inhibition, which resolves conflict between competing stimulus dimensions, and response inhibition, which suppresses prepotent motor responses (Luna et al., 2015; Nigg, 2000). These

components engage distinct neural substrates—interference inhibition activates the anterior cingulate cortex for conflict detection and the dorsolateral prefrontal cortex for control implementation (Botvinick et al., 2001), while response inhibition primarily recruits the right inferior frontal gyrus and pre-supplementary motor area (Aron et al., 2014). Converging evidence from behavioral, neuroimaging, and clinical studies supports both functional and developmental distinctions between these processes (Vuillier et al., 2016). Interference inhibition shows protracted development, with marked improvements between ages 7–10 and continued refinement into adolescence, whereas response inhibition demonstrates earlier competence (ages 4–5) with rapid gains through middle childhood (Cohen et al., 2016; Luna et al., 2015). Neuroimaging studies further reveal that these improvements correlate with distinct patterns of neural maturation: frontostriatal circuits for response inhibition and frontoparietal networks for interference inhibition (Madsen et al., 2010).

Despite compelling evidence for developmental dissociation, precise characterization of these trajectories remains elusive. Studies diverge regarding developmental timing, critical periods, and growth profiles—discrepancies that likely reflect methodological limitations. Previous research has either imposed predetermined growth models or relied on cross-sectional age group comparisons, potentially obscuring critical developmental patterns. To overcome these limitations, the field requires flexible analytical frameworks capable of accommodating complex, nonlinear patterns. Generalized Additive Models (GAM) with derivative analysis offer a promising solution by capturing nonlinear dynamics without imposing predetermined functional forms. This data-driven approach identifies periods of developmental acceleration

and deceleration through first derivatives (Tervo-Clemmens et al., 2023), revealing patterns that traditional methods may obscure. Yet systematic applications comparing interference and response inhibition trajectories remain limited—presenting an important opportunity to elucidate how these fundamental control processes develop and diverge across childhood and adolescence.

From Behavioral Indicators to Computational Mechanisms in Inhibitory Development

While conventional behavioral measures have provided foundational insights, they face significant limitations in characterizing the complex developmental dynamics of inhibitory control. Traditional paradigms quantify inhibitory capacity by comparing performance between conflict and baseline conditions, primarily through reaction time differences (interference effects) and accuracy rates (error rates). This approach, however, conflates multiple cognitive processes within single behavioral measures, potentially obscuring the precise mechanisms driving developmental change (Hedge et al., 2018; Rey-Mermet et al., 2018). For instance, identical interference effects may reflect either slow overall processing with intact conflict resolution or rapid processing with specific inhibitory deficits—distinct phenomena requiring different theoretical explanations.

Computational cognitive modeling offers a powerful solution by decomposing complex behavior into theoretically grounded component processes (Forstmann et al., 2016; Steinbeis & Crone, 2016). Rather than treating reaction times and accuracy as separate, isolated measures, computational models integrate multiple behavioral indicators within unified theoretical

frameworks. The Hierarchical Drift Diffusion Model (HDDM), grounded in evidence accumulation theory, exemplifies this approach by parsing decision-making into distinct cognitive operations (Forstmann et al., 2016). Recent developmental applications have yielded crucial insights. Ambrosi et al. (2019) applied diffusion modeling to interference tasks in children aged 5–11, revealing that age-related improvements stemmed primarily from enhanced drift rates rather than general slowing or strategic adjustments. This finding suggests that interference control develops through increasingly efficient conflict resolution rather than improved response caution. Similarly, Weigard et al. (2020) demonstrated that ADHD-related deficits in response inhibition were associated with reduced drift rates rather than lowered decision thresholds, challenging conventional interpretations of impulsivity as simply "acting without thinking." Furthermore, computational parameters demonstrate superior psychometric properties compared to traditional difference scores, exhibiting higher reliability and stronger correlations with external criteria (Lerche & Voss, 2017). By revealing latent cognitive processes, computational modeling can clarify whether interference and response inhibition share common developmental mechanisms or follow distinct paths—a question that traditional approaches have struggled to answer definitively.

Viewing Inhibitory Development through a Decision-Processing Lens

Despite surface differences in task demands and neural substrates, interference and response inhibition tasks share a core computational structure amenable to unified analysis through decision-making frameworks. Both task types require accumulation of evidence toward binary choice boundaries, a process precisely characterized by evidence accumulation

models (Bogacz et al., 2006). In *Stroop* tasks, participants accumulate evidence favoring word reading versus color naming until reaching a decision threshold. In *Go/No-Go* tasks, they continuously evaluate sensory evidence to determine whether stimuli match "Go" or "No-Go" criteria. This shared architecture of bounded evidence accumulation makes both task types ideally suited for drift diffusion modeling. HDDM provides a principled framework for decomposing these decision processes into their constituent components (Pan et al., 2025). Specifically, decision-makers continuously sample and integrate sensory information over time until accumulated evidence reaches a boundary that triggers response execution. This process can be disrupted by competing information (interference) or premature response tendencies (failed inhibition). HDDM captures these dynamics through four core parameters (see Supplementary Table S1), each mapping onto distinct cognitive-neural operations: First, drift rate (***v***) reflects the efficiency of evidence accumulation—the signal-to-noise ratio in information processing. Second, decision boundary separation (***a***) represents the amount of evidence required before committing to a response—the speed-accuracy trade-off setting. Third, starting point bias (***z***) captures systematic response preferences before stimulus onset. Finally, non-decision time (***t***) encompasses processes outside the decision itself: stimulus encoding, response execution, and control system engagement.

Integrating this computational framework with neurodevelopmental theory generates specific, testable predictions about inhibitory development. The conflict monitoring hypothesis suggests that interference inhibition depends critically on detecting conflict (anterior cingulate cortex) and implementing control (dorsolateral prefrontal cortex) (Botvinick et al., 2001).

Computationally, this should manifest as improvements in drift rate with age as conflict resolution becomes more efficient. Response inhibition, conversely, may depend more on strategically elevating decision boundaries (proactive control) or adjusting starting points away from prepotent response tendencies. Recent developmental applications support these predictions. Liu et al. (2022) found that improvements in Stroop performance from ages 6–12 were primarily associated with enhanced drift rates in incongruent trials, with minimal changes in decision boundaries or non-decision times. In contrast, Ratcliff et al. (2012) reported that *Go/No-Go* improvements from ages 8–15 stemmed from elevated decision boundaries and reduced non-decision times, with relatively stable drift rates. These findings suggest fundamentally different developmental mechanisms: interference control develops through enhanced evidence quality, while response inhibition develops through strategic control adjustments. These computational dissociations both support and extend theoretical models of inhibitory control architecture. The distinct patterns of drift rates and decision boundaries align with the view that interference and response inhibition rely on partially separable neural systems undergoing different maturational trajectories (Luna et al., 2015). Crucially, computational parameters provide the mechanistic precision missing from traditional "inhibition deficit" explanations. Rather than invoking vague notions of "poor inhibitory control," we can specify whether children struggle with evidence quality (drift rate), response caution (boundaries), or prepotent response regulation (starting point). These insights have direct implications for intervention: children with poor evidence accumulation may benefit from perceptual training, while those with boundary-setting difficulties may require strategy

instruction. By revealing the computational mechanisms underlying inhibitory development, this approach bridges the gap between neural development and behavioral change.

The Present Study

Building on this theoretical and methodological foundation, the first aim of this study was to characterize the developmental patterns of interference and response inhibition from childhood through adolescence. Based on multi-component executive function theory (Miyake et al., 2000; Nigg, 2000) and neurodevelopmental evidence (Luna et al., 2015), we expected both inhibitory components to show nonlinear development but with divergent trajectories. The second aim was to examine whether evidence accumulation models can account for developmental changes in these inhibitory subcomponents and identify the distinct computational mechanisms underlying their development.

To achieve these aims, we recruited participants aged 6–18—spanning the critical period from rapid development to stabilization (Christ et al., 2001). We first applied Generalized Additive Models (GAM) and Generalized Additive Mixed Models (GAMM) to characterize the nonlinear developmental patterns of behavioral performance without imposing predetermined functional forms. We then employed HDDM to decompose trial-level behavioral data into theoretically grounded computational processes and examined how these computational mechanisms mediate age-related changes in inhibitory control. By combining computational modeling with flexible developmental analysis, we aimed to provide a comprehensive understanding of how interference and response inhibition develop across childhood and adolescence.

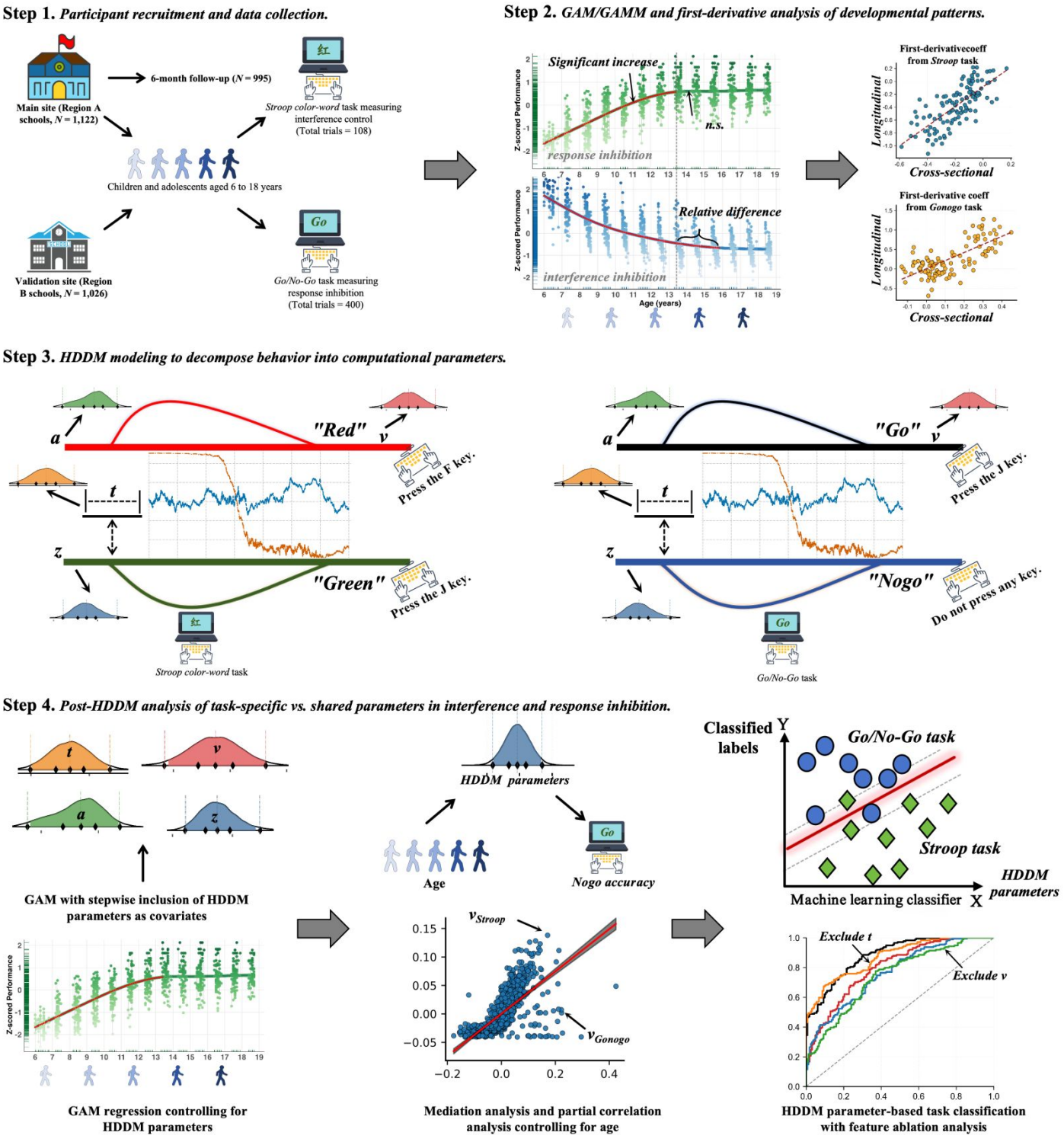

FIGURE 1. Experimental design flowchart.

***Note*: Step 1:** Participants from two sites (primary: $n = 1{,}122$ with longitudinal follow-up $n = 995$; replication: $n = 1{,}026$) completed *Stroop* and *Go/No-Go* tasks. **Step 2:** Developmental patterns were modeled using GAM (cross-sectional) and GAMM (longitudinal), with critical periods identified through derivative

analyses. **Step 3:** Task performance was decomposed into cognitive parameters using HDDM. **Step 4:** Cognitive mechanisms were examined through covariate analyses, mediation tests, partial correlations, and machine learning classification.

Method

Participants

We recruited 2,148 children and adolescents (aged 6 to 18 years) from schools across two regions in China. Participants were recruited from two independent sites: a primary site (n = 1,122; 45.54% female; M_{age} = 12.42 years, SD = 3.79 years, range: 6.0–18.7 years) with longitudinal follow-up, and a replication site (n = 1,026; 45.13% female; M_{age} = 12.44 years, SD = 3.77 years, range: 6.1–18.75 years) for cross-sectional validation of findings. Both samples were predominantly Han Chinese (primary: 91.9%; replication: 90.8%). The two sites demonstrated comparable demographic composition across all age groups (Supplementary Table S2) with no significant differences from the primary site in baseline distributions of inhibitory control indicators (all $p > 0.05$, Kolmogorov–Smirnov tests; Supplementary Figure S1). Data were collected between September 2022 and July 2024 in public schools in **[BLINDED FOR REVIEW]**. The study protocol was approved by the Ethics Committee of **[BLINDED FOR REVIEW]**.

To examine developmental stability over time, we conducted 6-month follow-up assessments exclusively with the primary site sample. Of the original 1,122 participants from the primary site, 995 (88.68%) completed follow-up testing. Attrition rates varied minimally across age groups, from 6.25% among 6-year-olds to 14.47% among 18-year-olds, with no

significant age-related differences (χ^2 = 5.92, p = 0.920). Importantly, attrition analyses revealed no selection bias: participants who completed follow-up did not differ from those lost to attrition on baseline Stroop interference (t = 0.83, p = 0.405) or Go/No-Go accuracy (t = 1.02, p = 0.307).

Parents or legal guardians provided written informed consent, and children gave verbal assent. All procedures followed the ethical principles of the Declaration of Helsinki. Inclusion criteria required participants to: (1) be native Mandarin Chinese speakers, (2) have normal or corrected-to-normal vision, (3) be free from parent-reported neurological disorders, psychiatric conditions, or cognitive developmental abnormalities, and (4) have no prior experience with similar cognitive tasks. We excluded children who were (1) taking medications known to affect cognitive function or (2) diagnosed with learning difficulties or attention-deficit/hyperactivity disorder. Participants received a small gift as compensation for their participation in the study.

Materials and Procedure

We assessed interference inhibition using a computerized adaptation of the **classical** *Stroop* paradigm (Stroop, 1935). The stimuli consisted of two high-frequency Chinese color words ("红" [red], "绿" [green]) and neutral symbols ("####"), presented centrally in either red or green ink (see Supplementary Figure S2). Participants identified the ink color while ignoring the word meaning, pressing "F" for red (left index finger) or "J" for green (right index finger). The task included three conditions: (a) congruent—word meaning matched ink color (e.g., "red" in red ink), (b) incongruent—word meaning conflicted with ink color (e.g., "green" in red ink), and (c) neutral—symbols without semantic content (e.g., "####" in red ink). The

Stroop interference effect, calculated as the reaction time difference between incongruent and congruent conditions, served as the primary measure of interference inhibition. Each trial followed a fixed sequence: fixation cross (500 ms) → blank screen (1,000 ms) → target stimulus (maximum 1500 ms) → inter-trial interval (500 ms). Following 18 practice trials with feedback, participants completed three blocks of 36 trials each (12 per condition), totaling 108 experimental trials. Conditions were pseudorandomized with no more than three consecutive trials of the same type. Participants achieving less than 85% accuracy during practice repeated the training until reaching this criterion. Self-paced rest breaks between blocks limited the total task duration to approximately 15 minutes. The Stroop interference effect demonstrated good internal consistency (Cronbach's $\alpha = 0.84$; Zhu et al., 2025).

Response inhibition was measured using a letter-based *Go/No-Go* paradigm (Gomez et al., 2007). Simple letter stimuli ("X" and "Y") minimized semantic processing demands. Participants responded rapidly to Go stimuli (target letters) while withholding responses to No-Go stimuli (non-targets) (Supplementary Figure S2). The brief stimulus duration (600 ms) and response window (400 ms) enhanced prepotent response tendencies, thereby increasing sensitivity to inhibitory control differences. The trial structure consisted of a fixation cross (1000 ms) → stimulus (600 ms) → blank response window (400 ms) → inter-trial interval (500 ms). To control for stimulus-specific confounds, we employed a counterbalanced target design across four blocks of 100 trials each (75% Go, 25% No-Go). Target assignments alternated between blocks: X served as the Go stimulus in blocks 1 and 3, Y in blocks 2 and 4. Block order was counterbalanced across participants using a Latin-square design. Following 20

practice trials with feedback (85% accuracy criterion), participants completed 400 experimental trials. The primary outcome measures included Go trial reaction time and accuracy, No-Go trial accuracy, and d-prime (d′), a signal detection measure of discriminability calculated as $d' = z$ (hit rate) $- z$ (false alarm rate). The task demonstrated high internal consistency (Cronbach's $\alpha = 0.88$) and required approximately 15 minutes to complete (Zhu et al., 2025).

The test took place in school computer laboratories using standardized equipment: 15.6-inch LED monitors (1600 × 900 resolution, 60 Hz refresh rate) positioned 60 cm away from participants. *E*-Prime 2.0 (Psychology Software Tools, Pittsburgh, PA) controlled stimulus presentation and recorded responses with millisecond-level precision. Trained graduate students in psychology administered all sessions following standardized protocols. After explaining the task requirements and demonstrating the procedures, experimenters confirmed participant understanding before beginning formal testing.

Data Analytic Strategy

Modeling Nonlinear Patterns and Identifying Critical Developmental Periods

We excluded participants whose reaction times exceeded three standard deviations above or below their age group means (Ambrosi et al., 2020). We then employed GAM for cross-sectional analyses and GAMM for longitudinal analyses (Tervo-Clemmens et al., 2023). These approaches use data-driven smooth functions to capture complex nonlinear developmental patterns without imposing predetermined functional forms, enabling detection of developmental accelerations, decelerations, and plateaus that traditional polynomial regression

might miss. For longitudinal analyses, GAMM incorporated random effects to account for within-participant dependencies (see Supplementary Methods for details). To identify periods of significant developmental change, we calculated the first derivatives of the fitted curves at 0.1-year intervals. Through 10,000 simulations, we generated simultaneous 95% confidence intervals for these derivatives. Significant developmental periods were defined as age ranges where confidence intervals consistently excluded zero, indicating reliable rates of change in inhibitory control abilities (Tervo-Clemmens et al., 2023).

Hierarchical Drift Diffusion Model Analysis

We employed the Hierarchical Drift Diffusion Model (HDDM version 1.0.1) implemented in Python to conduct computational modeling analysis of trial-level behavioral data from the *Stroop color-word* task and *Go/No-Go* task (Pan et al., 2025) aiming to examine the underlying computational mechanisms of inhibitory control processing (see Supplementary Methods for details). To decompose task performance into constituent cognitive processes, we implemented two hierarchical models. The baseline model included four core DDM parameters: decision boundary (***a***), drift rate (***v***), non-decision time (***t***), and starting point bias (***z***). This baseline specification assumed uniform parameter distributions across all experimental conditions and participant groups. Building upon this foundation, the age effect model incorporated age as a continuous predictor variable, allowing all core parameters to vary linearly with age to capture developmental patterns in cognitive control mechanisms (Zhang et al., 2025). We utilized the default prior distributions from the HDDM software package, which are derived from meta-analytic findings across extensive empirical research. These priors

provide an appropriate balance between conservatism to prevent overfitting and sufficient flexibility for parameters to adjust according to data characteristics (Zhang et al., 2025).

Parameter estimation was conducted within a hierarchical Bayesian framework, using Markov Chain Monte Carlo (MCMC) sampling methods to obtain posterior distributions. To ensure estimation reliability and reproducibility, each model was run with four independent MCMC chains, each containing 15,000 sampling iterations, with the first 5,000 samples discarded as burn-in. Between-chain convergence was verified using the Gelman-Rubin statistic ($\hat{R} < 1.01$) (Gelman et al., 2014). We assessed model performance through standard diagnostic procedures. Convergence was verified using the Gelman-Rubin statistic ($\hat{R} < 1.01$) and effective sample sizes (ESS > 400) (Pan et al., 2025). Model validity was evaluated through posterior predictive checks, comparing 500 simulated datasets with observed data at both individual and group levels (Peters & D'Esposito, 2020), which confirmed that the models adequately captured the empirical data patterns. Statistical inference followed a Bayesian framework. We used Bayes factors (BF_{10}) to quantify evidence strength for group differences and 95% Highest Density Intervals (HDI) to characterize parameter uncertainty within predetermined Regions of Practical Equivalence (ROPE) (Kruschke & Liddell, 2018; see Supplementary Methods).

Examining Computational Mechanisms Underlying Inhibitory Control

To reveal similarities and differences in the computational mechanisms underlying the two forms of inhibitory control, we analyzed parameter specificity and commonality. For parameter specificity analysis: (1) We employed a bootstrap mediation analysis framework

(3,000 bootstrap samples) to systematically examine the mediating role of HDDM parameters in the relationship between age and behavioral performance (Liu et al., 2022). (2) To quantify the explanatory contribution of HDDM parameters to developmental patterns, we constructed a series of nested GAM models, sequentially controlling for HDDM parameters. By comparing goodness-of-fit indices (Akaike Information Criterion, AIC) between models, we quantitatively assessed each parameter's explanatory power for developmental changes. For parameter commonality analysis: (1) We calculated partial correlations between corresponding parameters across tasks, while controlling for age effects. (2) We constructed a Support Vector Machine (SVM) classifier based on four core HDDM parameters to classify task type (*Stroop* vs. *Go/No-Go*) (see Supplementary Methods). Using feature ablation analysis, we systematically removed specific parameters and evaluated changes in classification performance, thereby quantifying each parameter's contribution to task discrimination.

Results

Developmental Patterns of Inhibitory Control from Ages 6–18

Nonlinear Patterns and Critical Developmental Periods with Cross-site Validation

To investigate the developmental patterns of inhibitory control, we applied GAM with penalized splines to fit cross-sectional data from children and adolescents aged 6–18 years. All GAM models showed nonlinear patterns (EDF > 4, all $p < 0.001$), rejecting linear developmental assumptions (Supplementary Table S3). To identify periods of significant change in inhibitory control abilities, we calculated first derivatives for each GAM model at 0.1-year intervals. Through simulation (10,000 iterations), we constructed confidence intervals

for first derivatives, evaluating statistical significance at each age point ($p < 0.05$ [two-sided] via simultaneous confidence intervals to account for multiple comparisons).

Analysis of developmental patterns revealed that inhibitory control abilities showed continuous but uneven age-related changes between ages 6 and 18, characterized by four distinct periods (Figure 2a, b; Supplementary Table S4): Early childhood rapid change (6–8 years): This period exhibited the steepest improvements across all measures, with annual gains ranging from 0.26 to 0.45 z-units (details in Supplementary Table S4). Both interference and response inhibition showed marked age-related improvements during these formative years. Pre-adolescent sustained growth (9–12 years): While developmental rates decelerated, steady progress continued. Improvements proceeded at approximately 50% of the early-phase rate for interference measures (0.23 z-units/year) and maintained robust gains for response inhibition indicators (0.31 z-units/year). Mid-adolescent deceleration (13–15 years): Further slowing characterized this transitional period, with all indicators showing modest but significant improvements (0.10–0.14 z-units/year), indicating development approaching cognitive stability. Late adolescent stabilization (16–18 years): Developmental changes ceased to reach statistical significance ($p > 0.05$ via simultaneous confidence intervals), indicating that inhibitory control abilities plateaued by age 16 within our observation window (Figure 2c). Interference inhibition and response inhibition demonstrated distinct developmental timelines. The significant developmental period for the Stroop incongruent condition extended to 15.8 years, representing 9.8 years of significant change (77.17% of the 12.7-year observation period). Response inhibition reached its plateau earlier, with No-Go accuracy and d' showing

342 significant changes only until 13.4 years, representing 7.4 years of significant change (58.27%
343 of the observation period). Bootstrap analysis confirmed that interference inhibition (Stroop
344 incongruent) and response inhibition (No-Go accuracy) differed significantly in their plateau
345 timing by 2.4 years (95% CI: [1.84, 2.96]; $p_{fdr} < 0.001$). The Stroop interference effect followed
346 an inverted U-shaped developmental pattern (Figure 2a, b).

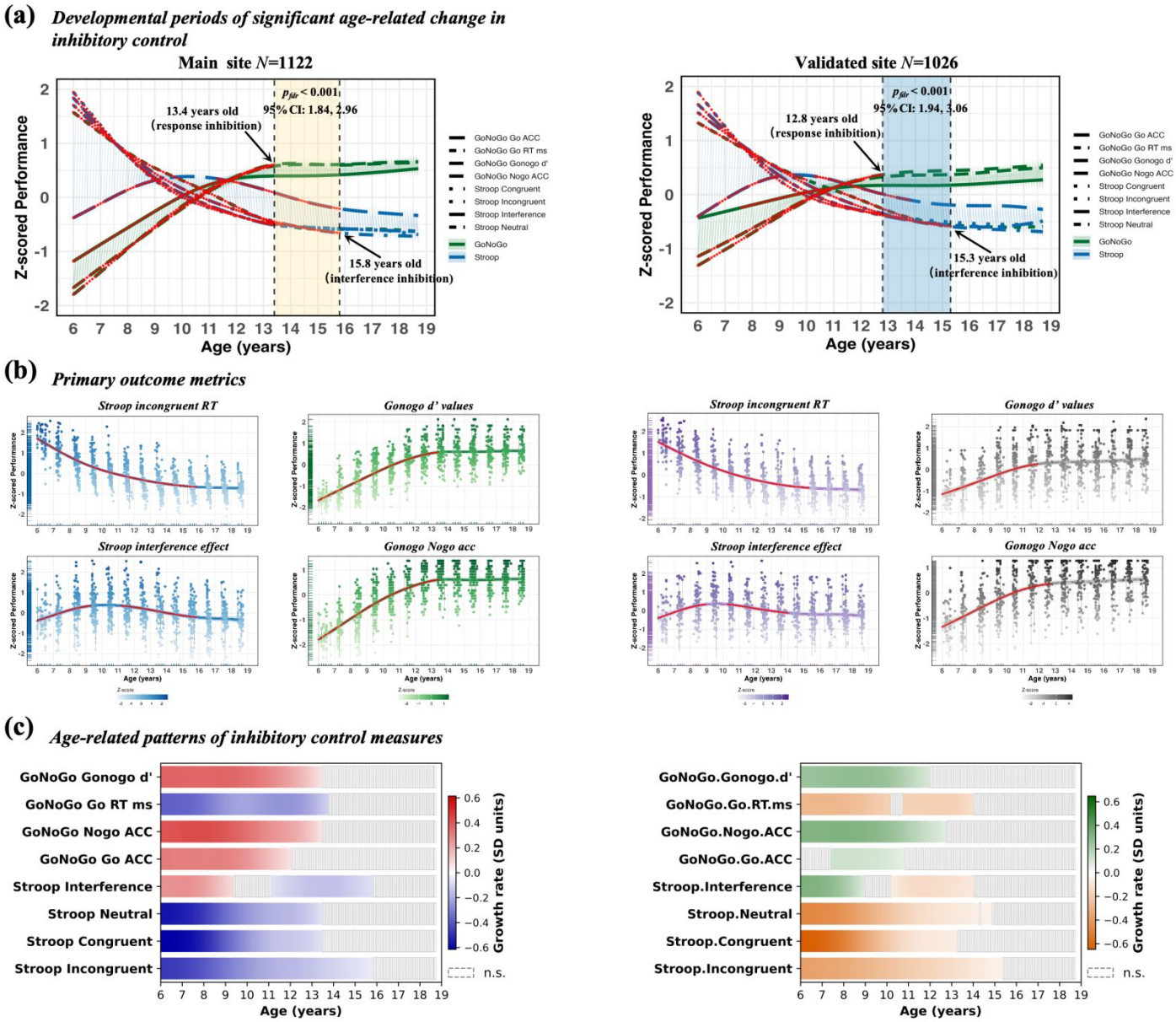

FIGURE 2. Developmental patterns of inhibitory control across primary and replication samples.

***Note*:** (**a**) GAM results with significant change periods highlighted. (**b**) Individual performance indicators with 95% CIs. (**c**) Heat maps of developmental change rates. Red/green = significant improvement; blue/orange = significant decline; white = non-significant change.

To verify the robustness and generalizability of our findings, we replicated the analyses using an independent replication sample. First, nonlinear developmental patterns characterized by four distinct periods were replicated (Supplementary Table S3). Second, the differential timing between interference and response inhibition was confirmed (Figure 2a, b). At the validation site, interference inhibition again showed significantly more protracted development than response inhibition (the Stroop incongruent condition showed significant changes until 15.3 years and the interference effect until 14.0 years, while No-Go accuracy plateaued at 12.8 years (53.54% of observation period) and d' at 12.1 years (48.03% of observation period; mean difference = 2.5 years, 95% CI: 1.94, 3.06; $p_{fdr} < 0.001$) (Figure 2c).

Longitudinal Validation with GAMM

To validate the developmental patterns through within-subject changes, we conducted 6-month follow-up assessments. Measurement stability was first established through age-detrended test–retest reliability (range: 0.648–0.964; Supplementary Figure S3), confirming stable individual differences after removing age-related trends. The longitudinal analyses validated our main cross-sectional findings (Figure 3a). First, the four-phase nonlinear

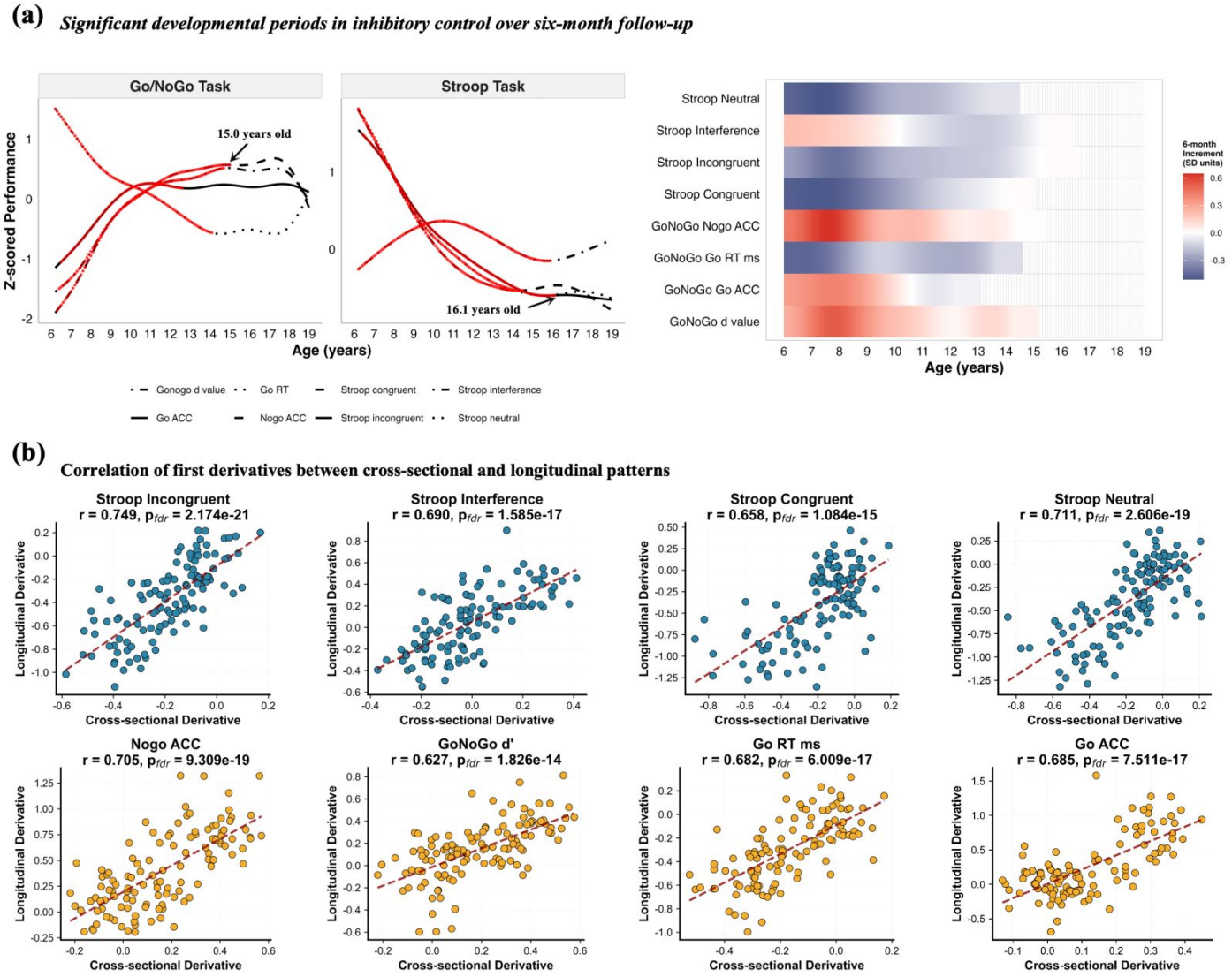

368 **FIGURE 3. Longitudinal validation of developmental patterns through 6-month follow-**

369 **up assessment.**

370 ***Note*: (a)** GAMM results showing developmental patterns (left) and change rate heat maps (right). Red =

371 significant improvement; blue = significant decline; white = non-significant change. (**b**) Correspondence

372 between cross-sectional (GAM) and longitudinal (GAMM) developmental estimates. Blue = interference

373 inhibition; orange = response inhibition.

374

developmental pattern was confirmed through GAMM (Supplementary Table S3, Table S4). Moreover, cross-sectional GAM and longitudinal GAMM derivatives showed strong concordance (r = 0.627–0.749, p_{fdr} < 0.001; Figure 3b), supporting the validity of the cross-sectional patterns. Second, differential developmental timing between interference and response inhibition was confirmed. The longitudinal data showed that interference inhibition had protracted development: the Stroop incongruent condition showed significant changes until 16.1 years (76.38% of observation period) and the interference effect until 15.9 years (76.38%). Response inhibition plateaued earlier: No-Go accuracy at 15.0 years (68.50%) and d' at 14.7 years (65.35%) (mean difference = 1.1 years, 95% CI: 0.54, 1.66; p_{fdr} < 0.001).

Distinct Computational Mechanisms for Interference and Response Inhibition

To identify the computational mechanisms distinguishing interference from response inhibition, we applied HDDM to trial-level behavioral data across both tasks. Model fitting showed excellent convergence (Supplementary Figure S4, Figure S5, and Table S5), allowing reliable parameter estimation (see Supplementary Results for details). Bayesian ANOVA revealed significant between-task differences in computational parameters. The drift rate was substantially higher in the *Stroop* task (95% HDI: 0.14–0.37; BF_{10} = inf; P(P|D) = 0.002; 0.3% in ROPE; see Figure 4a). This difference suggests more efficient evidence accumulation during interference resolution compared to response inhibition. Starting bias showed the opposite pattern, with lower values in the *Stroop* task relative to the *Go/No-Go* task (95% HDI: −0.46 to −0.41; BF_{10} = inf; P(P|D) < 0.001; 0.0% in ROPE). Decision boundaries were also lower in

the *Stroop* task compared to the *Go/No-Go* task (95% HDI: −0.32 to −0.067; BF_{10} = 10.24; P(P|D) = 0.089; 0.93% in ROPE). Non-decision time, however, showed no meaningful difference between tasks (95% HDI: −0.059 to 0.122; BF_{10} = 0.18; P(P|D) = 0.845; 94.0% in ROPE).

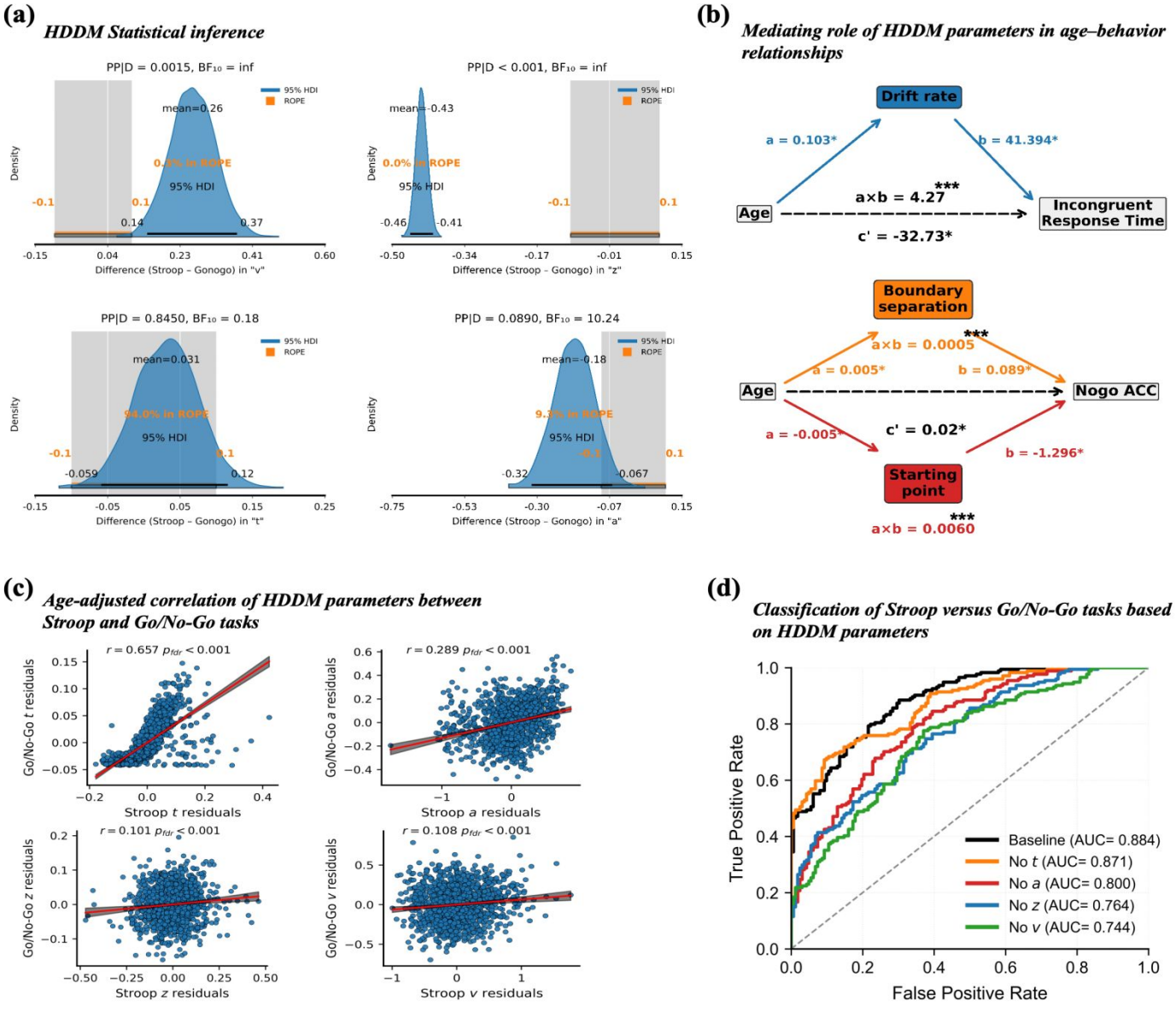

FIGURE 4. Dissociating task-specific and shared computational mechanisms underlying inhibitory control.

***Note*:** (**a**) Bayesian contrasts of HDDM parameters between *Stroop* and *Go/No-Go* tasks. (**b**) Mediation

analyses of HDDM parameters in age-related performance improvements. (**c**) Age-adjusted partial correlations between corresponding parameters across tasks. (**d**) SVM classification performance and feature importance through ablation analysis.

The mediation analysis revealed a significant negative association between age and incongruent trial reaction time (β = −28.46, $p < 0.001$; see Figure 4b), indicating improved conflict resolution ability across development. Among the four core HDDM parameters examined, drift rate (***v***) emerged as a significant mediator (indirect effect 95% CI [1.97, 6.56], $p < 0.001$), suggesting that age-related improvements in conflict processing speed are associated with enhanced efficiency in evidence accumulation. While decision boundary (***a***) increased significantly with age (β = 0.012, $p < 0.001$), reflecting developmental increases in response caution, its direct effect on reaction time was not significant (β = −25.46, $p = 0.221$), resulting in a non-significant indirect effect (95% CI [-0.88, 0.23], $p = 0.267$). The indirect effects of non-decision time (***t***) and starting bias (***z***) were similarly non-significant (0.40 and 0.13, respectively, $p > 0.22$), despite both parameters showing significant age-related changes.

The results for the *Go/No-Go* task revealed a contrasting pattern. Age positively predicted No-Go accuracy (β = 0.018, $p < 0.001$), reflecting developmental improvements in response inhibition. Unlike the *Stroop* task, starting bias (***z***) served as the primary mediator, accounting for 34.0% of the age effect. Specifically, age was associated with reduced starting bias (β = −0.005, $p < 0.001$), indicating a developmental decrease in prepotent "go" response tendencies. This bias reduction was significantly associated with enhanced No-Go accuracy through attenuating impulsive responses (β = -1.296, $p < 0.001$), yielding a significant positive indirect

effect (0.006, 95% CI [0.005, 0.007], $p < 0.001$). Decision boundary (***a***) demonstrated a significant but smaller mediating role, contributing 2.64% to the total effect. Age-related increases in decision criteria ($\beta = 0.005$, $p < 0.001$) were associated with improved task performance through more conservative responses ($\beta = 0.089$, $p < 0.001$), producing an indirect effect of 0.0005 (95% CI [0.0003, 0.0007], $p < 0.001$). Neither drift rate (***v***) nor non-decision time (***t***) showed significant mediating roles in the *Go/No-Go* task, consistent with the hypothesis of task-specific computational mechanisms underlying different forms of inhibitory control.

Moreover, our GAM analysis further quantified the relative contributions of each parameter to developmental patterns (Supplementary Table S6). In the *Stroop t*ask, controlling for drift rate (***v***) produced the largest decrease in model explanatory power ($\Delta R^2 = -0.128$, accounting for 24.5% of the original age effect). In the *Go/No-Go* task, controlling for starting bias (***z***) produced the largest decrease in explanatory power ($\Delta R^2 = -0.124$, accounting for 19.1%). Decision boundary (***a***) made moderate contributions in both tasks (*Stroop*: 12.6%; *Go/No-Go*: 14.2%). Non-decision time (***t***) also showed comparable contributions across tasks (*Stroop*: 10.3%; *Go/No-Go*: 10.8%). Notably, starting bias (***z***) had minimal effects on the *Stroop* task (2.3%), while drift rate (***v***) made limited contributions to the *Go/No-Go* task (5.1%). After controlling for all HDDM parameters simultaneously, the models accounted for approximately 40.2% and 35.5% of the age-related variance in *Stroop* and *Go/No-Go* performance, respectively. Importantly, nonlinear age effects in both tasks were no longer significant ($p > 0.05$).

To examine the shared and distinct mechanisms underlying HDDM parameters across different inhibitory control tasks, we conducted partial correlation analyses exploring the developmental associations of each parameter between the *Stroop* and *Go/No-Go* tasks. After controlling for age effects, non-decision time (***t***) showed the strongest cross-task association ($r = 0.680$, $p_{fdr} < 0.001$, $d = 1.854$) (Figure 4c). Decision boundary (a) exhibited a moderate but significant cross-task association ($r = 0.276$, $p_{fdr} < 0.001$, $d = 0.574$). In contrast, drift rate (***v***) and starting bias (***z***) showed pronounced task specificity. Notably, the cross-task association for drift rate decreased markedly when age was controlled (from $r = 0.364$, $p_{fdr} < 0.001$ in zero-order correlation to $r = 0.103$, pfdr = 0.001 in partial correlation). Similarly, starting bias demonstrated minimal cross-task association ($r = 0.095$, $p_{fdr} = 0.001$), further confirming the task-specific nature of response preparation strategies.

Additionally, to complement these correlational findings and quantify the degree of task specificity for each parameter, we employed SVM classifiers for feature importance analysis. The baseline model (including four parameters: a, v, t, and z) effectively distinguished between the *Stroop* and *Go/No-Go* tasks on the test set through 5-fold × 3-repeat nested cross-validation (area under the receiver operating characteristic curve [AUC] = 0.884) (Figure 4d). By systematically removing individual HDDM parameters, we revealed that drift rate (***v***) showed strong task discriminative ability: removing this parameter led to a significant decrease in classification performance (AUC = 0.744, ΔAUC = −0.110, $p_{fdr} = 0.004$). Removal of starting bias (***z***) similarly resulted in a significant decrease in classification performance (AUC = 0.764, ΔAUC = −0.120, $p_{fdr} = 0.004$). The pattern for decision boundary (***a***) and non-decision time (***t***)

revealed differential contributions to task classification. While the removal of decision boundary resulted in a statistically significant but relatively modest decrease in performance (AUC = 0.800, ΔAUC = −0.084, p_{fdr} = 0.008), the removal of non-decision time had virtually no impact on classifier performance (AUC = 0.871, ΔAUC = −0.013, p_{fdr} = 0.349).

Discussion

This study examined the developmental patterns and computational mechanisms of inhibitory control from ages 6-18 using cross-sectional (N = 2,148), replication, and longitudinal designs. To our knowledge, this represents the first study to provide computational evidence for both unity and diversity in inhibitory control development across childhood and adolescence through a decision-processing lens. We identified three key findings. First, both interference and response inhibition demonstrated nonlinear four-phase patterns—rapid improvement (6–8 years), sustained growth during pre-adolescence (9–12 years), deceleration in mid-adolescence (13–15 years), and stabilization in late adolescence (16–18 years). Second, these components exhibited distinct developmental trajectories, with response inhibition plateauing at 13.4 years while interference inhibition continued improving until 15.8 years—a 2.4-year difference that was consistently replicated across independent samples. Third, computational modeling revealed distinct underlying mechanisms: age-related changes in interference inhibition were primarily associated with enhanced drift rates ($\boldsymbol{v}$), reflecting improved conflict resolution efficiency, whereas age-related changes in response inhibition were linked to systematic adjustments in starting bias ($\boldsymbol{z}$), indicating strategic response

optimization. Both components showed shared improvements in non-decision time (***t***), suggesting common foundations in processing speed.

Nonlinear Development with Distinct Trajectories

Using GAM, we revealed that both interference and response inhibition demonstrated nonlinear developmental patterns from ages 6–18, characterized by four distinct phases. These findings align with previous investigations documenting nonlinear trajectories in executive function development during adolescence (Best & Miller, 2010; Luna et al., 2004), with recent large-scale cross-site analyses providing further corroboration (Tervo-Clemmens et al., 2023). As Diamond (2013) observed, improvements in childhood inhibitory ability correspond closely with maturation of prefrontal cortex structure and function, which undergoes substantial transitions during adolescence and exhibits pronounced nonlinear characteristics. By separately examining response inhibition and interference inhibition subcomponents, we found that both displayed nonlinear developmental patterns—a convergence that may reflect their shared neural substrates. Both functions primarily depend on prefrontal cortex activity, particularly functional integration between the right inferior frontal gyrus and anterior cingulate cortex. Neuroimaging evidence indicates that these brain regions undergo nonlinear structural and functional changes during childhood and adolescence, including complex trajectories in gray matter volume and progressive enhancement of white matter connectivity (Backhausen et al., 2022).

Crucially, through first-derivative analyses, we precisely characterized the developmental trajectories of inhibitory control subcomponents, revealing that interference inhibition

(extending to approximately 15.8 years) follows a more protracted developmental course than response inhibition (stabilizing around 13.4 years). This finding aligns with the developmental sequence framework proposed by Klenberg et al. (2001), wherein basic inhibitory functions (e.g., motor inhibition) typically emerge before more complex selective attention capabilities. Previous research has similarly documented differential patterns among inhibitory control subcomponents (Martin-Rhee & Bialystok, 2008; Tiego et al., 2018). For instance, studies have shown that *Go/No-Go* task performance reaches stability around age 12, whereas interference inhibition capacity in *Stroop* tasks continues improving from middle childhood through late adolescence (Leon-Carrion et al., 2004; Yeung et al., 2020). However, these earlier studies predominantly employed between-group comparisons, which limited continuous age analyses. The present investigation simultaneously assessed both inhibitory components within a large-scale sample, providing more precise developmental pattern estimates through continuous modeling and first-derivative analyses. This pattern of asynchronous development aligns with established neurodevelopmental findings and likely reflects differences in underlying neurobiological foundations. Response inhibition primarily engages the ventral prefrontal-basal ganglia circuit, which shows relatively rapid maturation during childhood (Casey et al., 2019; Luna et al., 2015). In contrast, interference inhibition requires coordinated integration across frontoparietal and salience networks, and these higher-order cognitive networks continue maturing into late adolescence (Luna et al., 2021). Electrophysiological evidence supports this distinction, revealing differential neural maturation patterns between these inhibitory components (Brydges et al., 2013). These researchers proposed that children's

diffuse pattern of frontal activation reflects ongoing neural network organization, requiring broader activation to accomplish task demands. This neural reorganization from diffuse to more focused activation patterns may represent a fundamental neurobiological mechanism underlying the protracted developmental trajectory of interference inhibition. Of particular interest, we observed a distinctive inverted U-shaped developmental trajectory for the Stroop interference effect, consistent with previous findings (Leon-Carrion et al., 2004). During early childhood (6–10 years), rapid reading automatization and semantic network expansion (Nation, 2017) increase children's sensitivity to semantic-color conflicts. However, their still-developing prefrontal executive control system (Diamond, 2013) limits their ability to inhibit prepotent responses, creating a critical gap between conflict detection and resolution. The anterior cingulate cortex (ACC), responsible for conflict monitoring, shows adult-like patterns by ages 8–10, whereas the dorsolateral prefrontal cortex (DLPFC), crucial for conflict resolution, continues maturing into late adolescence (Luna et al., 2015; Ordaz et al., 2013).

Computational Dissociation between Interference and Response Inhibition

This study represents the first computational investigation to simultaneously examine both the unity and diversity of inhibitory control across childhood and adolescence. Although numerous studies have explored developmental patterns of inhibitory control from multiple perspectives, existing research has remained primarily descriptive, offering limited insight into the underlying computational mechanisms that drive age-related changes (Hedge et al., 2018; Löffler et al., 2024; Luna et al., 2015). We addressed this gap by examining developmental patterns in inhibitory control through a computational decision-processing lens, extending the

application of drift diffusion models to investigate age-related changes across childhood and adolescence. Specifically, HDDM analysis of trial-level Stroop task data revealed that age-related improvements in interference inhibition were primarily associated with systematic increases in the drift rate parameter (***v***). Drift rate reflects the efficiency of evidence accumulation—the speed and quality with which individuals process stimulus information (Hedge et al., 2018). In the *Stroop* task, successful performance requires selecting relevant information from competing sources and resolving cognitive conflict; individuals must efficiently extract evidence supporting correct responses from conflicting information streams. This finding provides a mechanistic framework for understanding age-related improvements in interference inhibition. Children's prolonged reaction times appear closely related to differences in evidence accumulation processes (Ambrosi et al., 2019). Supporting this interpretation, Lewis et al. (2017) found that younger children are more prone to attentional lapses, which could impair their sampling efficiency of stimulus information and result in altered accumulation patterns.

In contrast to traditional research focusing solely on reaction times and accuracy, our findings suggest that age-related improvements in interference inhibition stem from enhanced cognitive conflict resolution processes rather than mere improvements in processing speed. From a neural perspective, age-related changes in drift rate likely reflect maturation of the prefrontal-anterior cingulate circuit. The anterior cingulate cortex monitors conflict while the dorsolateral prefrontal cortex implements resolution strategies; structural and functional changes in this circuit are associated with enhanced cognitive conflict processing efficiency

(Rueda et al., 2004). The more protracted developmental trajectory of interference inhibition compared to response inhibition may reflect the greater complexity of neural circuits underlying cognitive conflict resolution, which require extended periods to achieve full functional integration. For response inhibition, modeling analysis of the *Go/No-Go* task revealed that age-related improvements were primarily associated with systematic adjustments of the starting point bias parameter (z). The *Go/No-Go* task's asymmetric decision structure—with a high proportion of Go trials (requiring rapid responses) and a low proportion of No-Go trials (requiring response inhibition)—makes starting point position a particularly important strategic variable. In response inhibition tasks, information extraction processes are relatively straightforward and do not involve complex conflict resolution. Consequently, primary age-related changes manifest not in evidence extraction ability (drift rate), but rather in strategic aspects of decision-making. Behavioral differences traditionally interpreted as "inhibitory control ability" can be reconceptualized within the diffusion model framework as individual differences in starting point bias toward the "Go" boundary. This bias reflects strategic tendencies established before decision onset (Forstmann et al., 2016). Age-related changes in starting point bias suggest that with maturation, children and adolescents adopt increasingly flexible decision strategies when facing prepotent responses. This enhanced strategic adjustment ability likely reflects age-related improvements in prefrontal-mediated top-down control functions, enabling individuals to flexibly calibrate response tendencies according to task demands.

Despite these task-specific computational patterns, we identified an important shared foundation: the non-decision time parameter (***t***) exhibited significant age-related reductions in both tasks. Non-decision time encompasses cognitive processing outside the core decision process, including fundamental operations such as stimulus encoding, response preparation, and motor execution (Forstmann et al., 2016). This finding aligns with cognitive developmental theory, which posits that processing speed, as a foundational cognitive ability, supports higher-level cognitive functions. Supporting this interpretation, Löffler et al. (2024) demonstrated that when controlling for task-general processing components, task-specific executive function differences were substantially reduced. This suggests that individual differences in executive function performance may partially reflect variation in information processing speed. With maturation, improvements in children's information processing speed are associated with developmental changes throughout the central nervous system. These improvements in foundational abilities support higher cognitive functions such as working memory, contributing to performance gains across diverse cognitive domains (Kail, 2000).

A Decision-Computational Framework for Inhibitory Control Development

Collectively, our findings provide computational-level evidence that addresses the longstanding unity/diversity debate in inhibitory control. Building on these findings and recent theoretical developments (Löffler et al., 2024; Rey-Mermet et al., 2018; Simpson & Carroll, 2019), we propose a decision-computational framework that reconceptualizes developmental patterns of inhibitory control as systematic optimization of decision parameters rather than linear growth in a unitary ability (Figure 5). Within this framework, different inhibitory

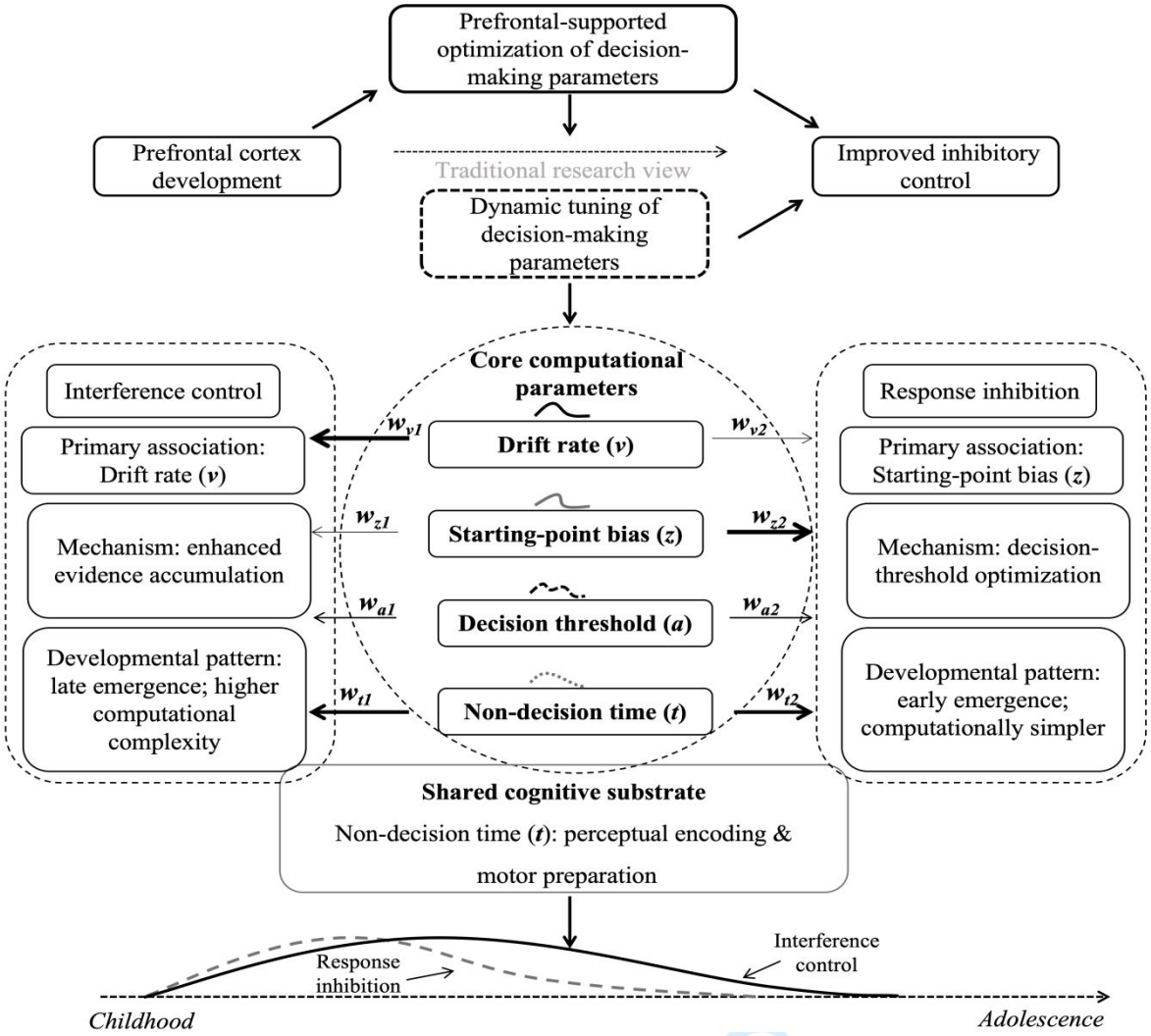

FIGURE 5. An integrative decision-computational framework for understanding developmental patterns of inhibitory control.

***Note*:** The framework illustrates task-specific optimization of decision parameters (drift rate for interference inhibition, starting bias for response inhibition) with shared foundations in processing speed improvements.

subcomponents optimize distinct computational parameters to meet specific task demands while sharing a common foundation in processing speed improvements. The framework comprises three core elements: (1) Task-specific mechanisms with shared foundations: Interference inhibition optimizes evidence accumulation (drift rate) to extract relevant signals

from competing information, while response inhibition adjusts decision thresholds (starting point bias) to balance speed-accuracy trade-offs. Both show consistent improvements in non-decision time, explaining moderate task intercorrelations (Friedman & Miyake, 2004) and supporting Löffler et al.'s (2024) findings that controlling for general processing substantially reduces task-specific differences. (2) Computational complexity drives developmental asynchrony: Interference inhibition's protracted trajectory reflects greater computational demands—requiring coordination among attention, conflict monitoring, and response selection networks. Response inhibition's simpler threshold calibration enables earlier stabilization. (3) Individual differences as computational strategies: Children may achieve similar behavioral outcomes through different computational routes—some enhancing drift rates (processing efficiency), while others adjust thresholds (response conservatism) (Ratcliff et al., 2012).

Limitations and Future Directions

Although this study provides novel evidence for understanding developmental patterns of inhibitory control in children and adolescents, several limitations warrant consideration. First, demographic variables remain insufficiently examined. While we identified a four-phase developmental pattern and documented asynchronous trajectories of inhibitory subcomponents, we did not systematically investigate how socioeconomic status, parental education, or family structure might moderate these patterns. Given compelling evidence that socioeconomic factors influence executive function development through their effects on prefrontal cortex structure and function (Yücel et al., 2012), future research should examine potential moderating

effects of these variables on the observed nonlinear trajectories. Second, extended longitudinal designs are essential for capturing true developmental dynamics. Although our 6-month follow-up provided preliminary validation of trajectory stability, understanding enduring changes in computational parameters requires substantially longer observation periods. Critical questions remain unanswered: Do different computational parameters change synchronously during rapid developmental periods? What characterizes parameter stability during plateau phases? How do individual differences in parameter optimization relate to long-term outcomes? Future research should implement longitudinal tracking spanning at least 2–3 years, with increased measurement density at critical developmental transitions. Such designs would enable more precise characterization of computational parameter dynamics and their temporal relationships with behavioral performance, while also allowing for examination of individual differences in developmental trajectories. Third, greater task diversity is needed to establish generalizability. While the *Stroop* and *Go/No-Go* tasks revealed distinct parameter patterns, whether these patterns generalize to other inhibitory control paradigms requires empirical validation. Given that different tasks may elicit distinct cognitive strategies and thus show different computational parameter contributions (Rey-Mermet et al., 2018), future research should employ a broader array of paradigms—including flanker tasks, stop-signal tasks, and antisaccade tasks—to evaluate parameter pattern consistency and specificity. Additionally, examining how computational parameters relate to real-world inhibitory demands would strengthen the ecological validity of these findings.

Conclusions and Implications

This study provides the first computational evidence for both unity and diversity in inhibitory control development across childhood and adolescence. By integrating flexible developmental modeling with computational approaches, we revealed that interference and response inhibition follow distinct developmental patterns associated with different computational mechanisms—enhanced evidence accumulation versus strategic threshold adjustments, respectively—while sharing improvements in non-decision time that reflect common foundations in processing speed. These findings advance a decision-computational framework that could transform inhibitory control from a descriptive construct into a mechanistically precise model of cognitive development.

Our findings carry significant implications for educational and clinical practice. In educational settings, the developmental gap between response inhibition and interference inhibition calls for age-specific instructional approaches. While basic classroom management may suffice for middle school students as response inhibition stabilizes, high school curricula should explicitly target interference control through activities that challenge students to reconcile competing information. In clinical contexts, computational parameter analysis enables more precise identification of specific deficits. For instance, children with ADHD may exhibit impaired drift rates (evidence accumulation) rather than boundary separation deficits (strategic control), pointing to fundamentally different intervention targets. This parameter-based approach not only provides nuanced diagnostic information but also guides targeted

interventions—perceptual training for evidence accumulation deficits versus metacognitive strategies for threshold-setting difficulties.

References

Allan, N. P., Hume, L. E., Allan, D. M., Farrington, A. L., & Lonigan, C. J. (2014). Relations between inhibitory control and the development of academic skills in preschool and kindergarten: A meta-analysis. *Developmental Psychology*, *50*(10), 2368. https://doi.org/10.1037/a0037493

Ambrosi, S., Servant, M., Blaye, A., & Burle, B. (2019). Conflict processing in kindergarten children: New evidence from distribution analyses reveals the dynamics of incorrect response activation and suppression. *Journal of Experimental Child Psychology*, *177*, 36–52. https://doi.org/10.1016/j.jecp.2018.06.006

Ambrosi, S., Śmigasiewicz, K., Burle, B., & Blaye, A. (2020). The dynamics of interference control across childhood and adolescence: Distribution analyses in three conflict tasks and ten age groups. *Developmental Psychology*, *56*(12), 2262–2280. https://doi.org/10.1037/dev0001122

Aron, A. R., Robbins, T. W., & Poldrack, R. A. (2014). Inhibition and the right inferior frontal cortex: One decade on. *Trends in Cognitive Sciences*, *18*(4), 177–185. https://doi.org/10.1016/j.tics.2013.12.003

Backhausen, L. L., Herting, M. M., Tamnes, C. K., & Vetter, N. C. (2022). Best practices in structural neuroimaging of neurodevelopmental disorders. *Neuropsychology Review*, *32*(2), 400–418. https://doi.org/10.1007/s11065-021-09496-2

Beauchamp, M. H., & Anderson, V. (2010). SOCIAL: an integrative framework for the development of social skills. *Psychological Bulletin*, *136*(1), 39. https://doi.org/10.1037/a0017768

Best, J. R., & Miller, P. H. (2010). A developmental perspective on executive function. *Child Development*, *81*(6), 1641–1660. https://doi.org/10.1111/j.1467-8624.2010.01499.x

Bogacz, R., Brown, E., Moehlis, J., Holmes, P., & Cohen, J. D. (2006). The physics of optimal decision making: A formal analysis of models of performance in two-alternative forced-choice tasks. *Psychological Review*, *113*(4), 700–765. https://doi.org/10.1037/0033-295X.113.4.700

Botvinick, M. M., Braver, T. S., Barch, D. M., Carter, C. S., & Cohen, J. D. (2001). Conflict monitoring and cognitive control. *Psychological Review*, *108*(3), 624. https://doi.org/10.1037/0033-295X.108.3.624

Brydges, C. R., Anderson, M., Reid, C. L., & Fox, A. M. (2013). Maturation of cognitive control: Delineating response inhibition and interference suppression. *PloS One*, *8*(7), e69826. https://doi.org/10.1371/journal.pone.0069826

Casey, B. J., Heller, A. S., Gee, D. G., & Cohen, A. O. (2019). Development of the emotional brain. *Neuroscience Letters*, *693*, 29–34. https://doi.org/10.1016/j.neulet.2017.11.055

Cataldo, A. M., Scheuer, L., Maksimovskiy, A. L., Germine, L. T., & Dillon, D. G. (2023). Abnormal evidence accumulation underlies the positive memory deficit in depression. *Journal of Experimental Psychology: General*, *152*(1), 139–156. https://doi.org/10.1037/xge0001268

Christ, S. E., White ,Desiree A., Mandernach ,Tammy, & and Keys, B. A. (2001). Inhibitory Control Across the Life Span. *Developmental Neuropsychology*, *20*(3), 653–669. https://doi.org/10.1207/S15326942DN2003_7

Cohen, A. O., Breiner, K., Steinberg, L., Bonnie, R. J., Scott, E. S., Taylor-Thompson, K., Rudolph, M. D., Chein, J., Richeson, J. A., & Heller, A. S. (2016). When is an adolescent an adult? Assessing cognitive control in emotional and nonemotional contexts. *Psychological Science*, *27*(4), 549–562. https://doi.org/10.1177/0956797615627625

Diamond, A. (2013). Executive Functions. *Annual Review of Psychology*, *64*(1), 135–168. https://doi.org/10.1146/annurev-psych-113011-143750

Forstmann, B. U., Ratcliff, R., & Wagenmakers, E.-J. (2016). Sequential Sampling Models in Cognitive Neuroscience: Advantages, Applications, and Extensions. *Annual Review of Psychology*, *67*(Volume 67, 2016), 641–666. https://doi.org/10.1146/annurev-psych-122414-033645

Friedman, N. P., & Miyake, A. (2004). The Relations Among Inhibition and Interference Control Functions: A Latent-Variable Analysis. *Journal of Experimental Psychology: General*, *133*(1), 101–135. https://doi.org/10.1037/0096-3445.133.1.101

Gelman, A., Hwang, J., & Vehtari, A. (2014). Understanding predictive information criteria for Bayesian models. *Statistics and Computing*, *24*(6), 997–1016. https://doi.org/10.1007/s11222-013-9416-2

744 Gomez, P., Ratcliff, R., & Perea, M. (2007). A model of the go/no-go task. *Journal of*
745 *Experimental Psychology: General*, *136*(3), 389. https://doi.org/10.1037/0096-
746 3445.136.3.389
747 Hedge, C., Powell, G., Bompas, A., Vivian-Griffiths, S., & Sumner, P. (2018). Low and
748 variable correlation between reaction time costs and accuracy costs explained by
749 accumulation models: Meta-analysis and simulations. *Psychological Bulletin*, *144*(11),
750 1200–1227. https://doi.org/10.1037/bul0000164
751 Kail, R. (2000). Speed of Information Processing: Developmental Change and Links to
752 Intelligence. *Journal of School Psychology*, *38*(1), 51–61. https://doi.org/10.1016/S0022-
753 4405(99)00036-9
754 Klenberg, L., Korkman, M., & Lahti-Nuuttila, P. (2001). Differential Development of
755 Attention and Executive Functions in 3- to 12-Year-Old Finnish Children. *Developmental*
756 *Neuropsychology*, *20*(1), 407–428. https://doi.org/10.1207/S15326942DN2001_6
757 Kruschke, J. K., & Liddell, T. M. (2018). The Bayesian New Statistics: Hypothesis testing,
758 estimation, meta-analysis, and power analysis from a Bayesian perspective. *Psychonomic*
759 *Bulletin & Review*, *25*(1), 178–206. https://doi.org/10.3758/s13423-016-1221-4
760 Leon-Carrion, J., García-Orza, J., & Pérez-Santamaría, F. J. (2004). Development of the
761 inhibitory component of the executive functions in children and adolescents. *International*
762 *Journal of Neuroscience*, *114*(10), 1291–1311.
763 https://doi.org/10.1080/00207450490476066

764 Lerche, V., & Voss, A. (2017). Retest reliability of the parameters of the Ratcliff diffusion
765 model. *Psychological Research*, *81*, 629–652. https://doi.org/10.1007/s00426-016-0770-
766 5
767 Lewis, F. C., Reeve, R. A., Kelly, S. P., & Johnson, K. A. (2017). Evidence of substantial
768 development of inhibitory control and sustained attention between 6 and 8 years of age on
769 an unpredictable Go/No-Go task. *Journal of Experimental Child Psychology*, *157*, 66–80.
770 https://doi.org/10.1016/j.jecp.2016.12.008
771 Liu, T., Wang, D., Wang, C., Xiao, T., & Shi, J. (2022). The influence of reward anticipation
772 on conflict control in children and adolescents: Evidences from hierarchical drift-diffusion
773 model and event-related potentials. *Developmental Cognitive Neuroscience*, *55*, 101118.
774 https://doi.org/10.1016/j.dcn.2022.101118
775 Löffler, C., Frischkorn, G. T., Hagemann, D., Sadus, K., & Schubert, A.-L. (2024). The
776 common factor of executive functions measures nothing but speed of information uptake.
777 *Psychological Research*, *88*(4), 1092–1114. https://doi.org/10.1007/s00426-023-01924-7
778 Luna, B., Garver, K. E., Urban, T. A., Lazar, N. A., & Sweeney, J. A. (2004). Maturation of
779 Cognitive Processes From Late Childhood to Adulthood. *Child Development*, *75*(5),
780 1357–1372. https://doi.org/10.1111/j.1467-8624.2004.00745.x
781 Luna, B., Marek, S., Larsen, B., Tervo-Clemmens, B., & Chahal, R. (2015). An Integrative
782 Model of the Maturation of Cognitive Control. *Annual Review of Neuroscience*,
783 *38*(Volume 38, 2015), 151–170. https://doi.org/10.1146/annurev-neuro-071714-034054

784 Luna, B., Tervo-Clemmens, B., & Calabro, F. J. (2021). Considerations when characterizing
785 adolescent neurocognitive development. *Biological Psychiatry*, *89*(2), 96–98.
786 https://doi.org/10.1016/j.biopsych.2020.04.026
787 Madsen, K. S., Baaré, W. F., Vestergaard, M., Skimminge, A., Ejersbo, L. R., Ramsøy, T. Z.,
788 Gerlach, C., Åkeson, P., Paulson, O. B., & Jernigan, T. L. (2010). Response inhibition is
789 associated with white matter microstructure in children. *Neuropsychologia*, *48*(4), 854–
790 862. https://doi.org/10.1016/j.neuropsychologia.2009.11.001
791 Martin-Rhee, M. M., & Bialystok, E. (2008). The development of two types of inhibitory
792 control in monolingual and bilingual children. *Bilingualism: Language and Cognition*,
793 *11*(1), 81–93. https://doi.org/10.1017/S1366728907003227
794 Miyake, A., Friedman, N. P., Emerson, M. J., Witzki, A. H., Howerter, A., & Wager, T. D.
795 (2000). The Unity and Diversity of Executive Functions and Their Contributions to
796 Complex "Frontal Lobe" Tasks: A Latent Variable Analysis. *Cognitive Psychology*, *41*(1),
797 49–100. https://doi.org/10.1006/cogp.1999.0734
798 Nation, K. (2017). Nurturing a lexical legacy: Reading experience is critical for the
799 development of word reading skill. *Npj Science of Learning*, *2*(1), 3.
800 https://doi.org/10.1038/s41539-017-0004-7
801 Nigg, J. T. (2000). On inhibition/disinhibition in developmental psychopathology: Views from
802 cognitive and personality psychology and a working inhibition taxonomy. *Psychological*
803 *Bulletin*, *126*(2), 220–246. https://doi.org/10.1037/0033-2909.126.2.220

804 Nigg, J. T. (2017). Annual Research Review: On the relations among self-regulation,
805 self-control, executive functioning, effortful control, cognitive control, impulsivity,
806 risk-taking, and inhibition for developmental psychopathology. *Journal of Child*
807 *Psychology and Psychiatry*, *58*(4), 361–383. https://doi.org/10.1111/jcpp.12675
808 Nigg, J. T., Jester, J. M., Stavro, G. M., Ip, K. I., Puttler, L. I., & Zucker, R. A. (2017).
809 Specificity of executive functioning and processing speed problems in common
810 psychopathology. *Neuropsychology*, *31*(4), 448–466.
811 https://doi.org/10.1037/neu0000343
812 Ordaz, S. J., Foran, W., Velanova, K., & Luna, B. (2013). Longitudinal Growth Curves of
813 Brain Function Underlying Inhibitory Control through Adolescence. *Journal of*
814 *Neuroscience*, *33*(46), 18109–18124. https://doi.org/10.1523/JNEUROSCI.1741-13.2013
815 Pan, W., Geng, H., Zhang, L., Fengler, A., Frank, M. J., Zhang, R.-Y., & Chuan-Peng, H.
816 (2025). dockerHDDM: A User-Friendly Environment for Bayesian Hierarchical Drift-
817 Diffusion Modeling. *Advances in Methods and Practices in Psychological Science*.
818 https://doi.org/doi.org/10.1177/2515245924129
819 Peters, J., & D'Esposito, M. (2020). The drift diffusion model as the choice rule in inter-
820 temporal and risky choice: A case study in medial orbitofrontal cortex lesion patients and
821 controls. *PLOS Computational Biology*, *16*(4), e1007615.
822 https://doi.org/10.1371/journal.pcbi.1007615

Ratcliff, R., Love, J., Thompson, C. A., & Opfer, J. E. (2012). Children Are Not Like Older Adults: A Diffusion Model Analysis of Developmental Changes in Speeded Responses. *Child Development*, *83*(1), 367–381. https://doi.org/10.1111/j.1467-8624.2011.01683.x

Rey-Mermet, A., Gade, M., & Oberauer, K. (2018). Should we stop thinking about inhibition? Searching for individual and age differences in inhibition ability. *Journal of Experimental Psychology: Learning, Memory, and Cognition*, *44*(4), 501–526. https://doi.org/10.1037/xlm0000450

Rueda, M. R., Posner, M. I., Rothbart, M. K., & Davis-Stober, C. P. (2004). Development of the time course for processing conflict: An event-related potentials study with 4 year olds and adults. *BMC Neuroscience*, *5*, 1–13. https://doi.org/10.1186/1471-2202-5-39

Simpson, A., & Carroll, D. J. (2019). Understanding early inhibitory development: Distinguishing two ways that children use inhibitory control. *Child Development*, *90*(5), 1459–1473. https://doi.org/10.1111/cdev.13283

Steinbeis, N., & Crone, E. A. (2016). The link between cognitive control and decision-making across child and adolescent development. *Current Opinion in Behavioral Sciences*, *10*, 28–32. https://doi.org/10.1016/j.cobeha.2016.04.009

Stroop, J. R. (1935). Studies of interference in serial verbal reactions. *Journal of Experimental Psychology*, *18*(6), 643–662. https://doi.org/10.1037/h0054651

Tervo-Clemmens, B., Calabro, F. J., Parr, A. C., Fedor, J., Foran, W., & Luna, B. (2023). A canonical trajectory of executive function maturation from adolescence to adulthood. *Nature Communications*, *14*(1), 6922. https://doi.org/10.1038/s41467-023-42540-8

Tiego, J., Testa, R., Bellgrove, M. A., Pantelis, C., & Whittle, S. (2018). A Hierarchical Model of Inhibitory Control. *Frontiers in Psychology*, *9*. https://doi.org/10.3389/fpsyg.2018.01339

Vehtari, A., Gelman, A., & Gabry, J. (2017). Practical Bayesian model evaluation using leave-one-out cross-validation and WAIC. *Statistics and Computing*, *27*(5), 1413–1432. https://doi.org/10.1007/s11222-016-9696-4

Vuillier, L., Bryce, D., Szücs, D., & Whitebread, D. (2016). The Maturation of Interference Suppression and Response Inhibition: ERP Analysis of a Cued Go/Nogo Task. *PLOS ONE*, *11*(11), e0165697. https://doi.org/10.1371/journal.pone.0165697

Weigard, A., Soules, M., Ferris, B., Zucker, R. A., Sripada, C., & Heitzeg, M. (2020). Cognitive Modeling Informs Interpretation of Go/No-Go Task-Related Neural Activations and Their Links to Externalizing Psychopathology. *Biological Psychiatry: Cognitive Neuroscience and Neuroimaging*, *5*(5), 530–541. https://doi.org/10.1016/j.bpsc.2019.11.013

Yeung, M. K., Lee, T. L., & Chan, A. S. (2020). Neurocognitive development of flanker and Stroop interference control: A near-infrared spectroscopy study. *Brain and Cognition*, *143*, 105585. https://doi.org/10.1016/j.bandc.2020.105585

Yücel, M., Fornito, A., Youssef, G., Dwyer, D., Whittle, S., Wood, S. J., Lubman, D. I., Simmons, J., Pantelis, C., & Allen, N. B. (2012). Inhibitory control in young adolescents: The role of sex, intelligence, and temperament. *Neuropsychology*, *26*(3), 347–356. https://doi.org/10.1037/a0027693

Zhang, T., Yang, X., Mu, P., Huo, X., & Zhao, X. (2025). Stage-specific computational mechanisms of working memory deficits in first-episode and chronic schizophrenia. *Schizophrenia Research*, *282*, 203–213. https://doi.org/10.1016/j.schres.2025.06.012

Zhu, X., Tang, Y., Wang, S., Ma, X., Lin, J., Chai, Q., Yang, X., & Zhao, X. (2025). Underlying mechanisms in the relationship between family socioeconomic status and mathematical abilities: A longitudinal investigation. *Cognitive Development*, *75*, 101591. https://doi.org/10.1016/j.cogdev.2025.101591

Supplementary materials

Table of contents

Supplementary Methods and Results

GAM and GAMM Model Specifications

For cross-sectional analyses, we implemented GAM (Formula 1), incorporating an intercept term and using penalized thin plate regression splines to model age effects:

Formula 1: $Y_i = \beta_0 + f(\text{age}_i) + \varepsilon_i$

where Y_i represents the inhibitory control measure for participant i, β_0 denotes the intercept, $f(\text{age}_i)$ represents the smooth function of age using thin plate regression splines, and ε_i is the normally distributed error term.

For longitudinal analyses, we employed GAMM (Formula 2) to account for within-participant dependencies, incorporating random intercepts and slopes alongside the nonlinear age function:

Formula 2: $Y_{ij} = \beta_0 + u_{0j} + (u_{1j} \times \text{age}_{ij}) + f(\text{age}_{ij}) + \varepsilon_{ij}$

where Y_{ij} represents the outcome measure for participant j at timepoint i, u_{0j} and u_{1j} denote random intercept and slope for participant j, respectively, $f(\text{age}_{ij})$ represents the population-level smooth age function, and $\sigma^2 u_0$ and $\sigma^2 u_1$ represent the variances of random intercept and slope terms.

Hierarchical DDM analysis

***HDDM Specifications*:** For the *Stroop* task, model input data included participant ID, trial number, age group, response type (0 = "F" key press for red, 1 = "J" key press for green), and reaction time in milliseconds. Following established *Stroop* task analysis procedures (Ambrosi et al., 2020), we included only correct response trials in the analysis to ensure that the model parameter estimates reflected successful cognitive control processes. For the *Go/No-Go* task, although this paradigm includes the option of withholding responses, behavioral performance can be effectively modeled within the DDM framework (Gorka et al., 2023; Ratcliff et al., 2018). We implemented the stimulus-coded DDM approach (https://hddm.readthedocs.io/en/latest/tutorial_regression_stimcoding.html), conceptualizing the task as a binary stimulus classification decision process in which participants determined whether the presented stimulus belonged to the Go or No-Go category. In this parameterization, the upper boundary (1) represented the "Go" classification decision, while the lower boundary (0) represented the "No-Go" classification decision. Drift rates were specified as $+\boldsymbol{v}$ (Go decision) and $-\boldsymbol{v}$ (No-Go decision) to reflect opposing rates of evidence accumulation toward each response option. Given the higher frequency of Go stimuli (75%), the model incorporated a starting point bias parameter (z) to capture participants' prior expectation favoring Go responses (Letkiewicz et al., 2024). For data coding, correct key press responses on Go trials were coded as 1, while successful inhibitions on No-Go trials were coded as 0. Following HDDM documentation guidelines (https://hddm.readthedocs.io/en/latest/tutorial_gonogo_chisquare.html), reaction times for

correct inhibitions were coded as "999," while reaction times for incorrect key presses on No-Go trials were coded as "-999" (Letkiewicz et al., 2024; Yang & van Vugt, 2025). To account for potential outliers and response contamination, we designated 5% of trials as potential outliers (*p_outlier* = 0.05), which is consistent with established practices for controlling trials that may not follow the standard drift diffusion process (Letkiewicz et al., 2024).

***HDDM Statistical inference*:** We used Bayes factors for statistical inference, following the interpretation criteria established by Dienes (2016). Evidence supporting the alternative hypothesis was considered weak when $1 < BF_{10} < 3$, and evidence supporting the null hypothesis was considered weak when $1/3 < BF_{10} < 1$. Moderate evidence was defined as $3 < BF_{10} < 10$ (supporting the alternative hypothesis) or $1/10 < BF_{10} < 1/3$ (supporting the null hypothesis). Strong evidence supporting the alternative hypothesis was indicated by $BF_{10} > 10$, while strong evidence supporting the null hypothesis was indicated by $BF_{10} < 1/10$. To evaluate the practical significance of parameter estimates, we examined the relation between the 95% highest density interval (HDI) and the region of practical equivalence (ROPE) (Szul et al., 2020). When the 95% HDI fell entirely outside the ROPE, we considered the parameter to be credibly different from zero. When the 95% HDI fell entirely within the ROPE, the parameter was considered practically equivalent to zero. For cases where the 95% HDI partially overlapped with the ROPE, we calculated the Bayesian posterior probability (P|D). To distinguish between Bayesian posterior probabilities and classical frequentist p-values, we denoted frequentist p-values as p and Bayesian posterior probabilities as P|D. The interpretation of P|D followed established criteria (Szul et al., 2020): when P|D = 1, the ROPE was completely

contained within the 95% HDI, leading to acceptance of the null hypothesis (parameters were considered equivalent across conditions). When P|D = 0, the ROPE fell completely outside the 95% HDI, leading to rejection of the null hypothesis (parameters differed across conditions). When 0 < P|D < 1, the ROPE and 95% HDI partially overlapped, with the P|D value representing the proportion of the 95% HDI within the ROPE, indicating the probability that parameters were practically equivalent across conditions (Kruschke & Liddell, 2018).

Machine Learning Classifier Procedures

Machine learning analyses were conducted using *Python* (version 3.10.11) and the scikit-learn package (version 1.3.0). To ensure model reliability and generalizability, we divided the dataset into training and test sets using stratified sampling, with proportions of 70% and 30%, respectively (Schultebraucks et al., 2022; Webb et al., 2020). This approach preserved the proportions of different categories in each subset consistent with those in the original dataset. Model training employed a 5×3 nested cross-validation strategy to optimize performance and prevent overfitting. The implementation process was as follows: the training set was divided into five equal subsets as outer folds, with each outer subset further divided into three parts as inner folds. Inner cross-validation was used for hyperparameter optimization, utilizing the Optuna algorithm for automated parameter search (Akiba et al., 2019). During each inner validation, two subsets (comprising 2/3 of the inner data) were used for model training, with the remaining subset (1/3) used for model validation. This process was repeated three times to determine the optimal hyperparameter configuration for each outer fold. After determining optimal parameters, outer cross-validation used four folds for model training and the remaining

fold for performance evaluation. This process was repeated five times to complete the nested cross-validation procedure. Based on the optimal parameter combinations identified through nested cross-validation, we trained the final model on the complete training set (70% of data) without further parameter adjustments. Following model training, evaluation was conducted once on the independent test set (30% of data) to assess the model's generalization performance on unseen data (Habets et al., 2023).

HDDM fitting performance

MCMC chain trace plots showed that all parameters achieved convergence, with Gelman-Rubin statistics ($\hat{R}$) satisfying convergence criteria (Supplementary Figure S4, Table S5), indicating stable model fitting. While some parameters showed $\hat{R}$ values slightly above 1.01, all remained below 1.02 with sufficient effective sample sizes (bulk ESS > 400), meeting current practice recommendations (Pan et al., 2025). Posterior predictive checks further supported model adequacy: simulated data generated from parameter posterior distributions were essentially consistent with the observed data in distribution characteristics at both the individual and group levels (Supplementary Figure S5).

Supplementary Tables

Supplementary Table S1. Computational parameters of the drift diffusion model and their functional significance in cognitive processing.

Parameter	Cognitive Processing Description
a boundary separation	Represents the amount of evidence required to distinguish between "respond" and "inhibit" decisions, reflecting response caution in inhibitory control. Higher boundary separation values indicate more conservative decision criteria, whereby individuals require greater evidence accumulation before initiating a response, demonstrating enhanced cognitive control.
v drift rate	Reflects the rate of evidence accumulation over time, indicating information processing efficiency during conflict situations. Higher drift rates suggest more effective extraction of task-relevant information and suppression of irrelevant interference, demonstrating proficient conflict monitoring and resolution capabilities.
t non-decision time	Encompasses perceptual and motor processing duration, including stimulus encoding and response execution. This parameter captures the fundamental efficiency of perceptual-motor processes, spanning non-decisional components such as visual encoding, motor preparation, and response implementation.
z starting point bias	Indicates the initial position of evidence accumulation, reflecting systematic response tendencies. Bias toward a particular decision boundary suggests response predispositions, which may be influenced by task strategies, stimulus probabilities, or prior experience.

***Note*:** Parameter definitions are adapted from (Ratcliff et al., 2016).

130 **Supplementary Table S2. Participant demographic characteristics.**

	Primary Sample (N = 1,122) *				Validation Sample (N = 1,026)			
Age (Group)	*n*	Males, *n* (%)	Age, *M* ± SD	Ethnic, Han, *n* (%)	*n*	Males, *n* (%)	Age, *M* ± SD	Ethnic, Han, *n* (%)
6	80	43 (53.75%)	6.41 ± 0.23	73 (91.3%)	72	38 (52.78%)	6.44 ± 0.22	63 (87.5%)
7	92	47 (51.09%)	7.34 ± 0.19	83 (90.2%)	84	48 (57.14%)	7.32 ± 0.20	77 (91.7%)
8	98	52 (53.06%)	8.46 ± 0.17	93 (94.9%)	90	50 (55.56%)	8.45 ± 0.23	81 (90.0%)
9	90	50 (55.56%)	9.48 ± 0.20	83 (92.2%)	82	46 (56.10%)	9.52 ± 0.21	73 (89.0%)
10	87	46 (52.87%)	10.47 ± 0.17	77 (88.5%)	80	44 (55.00%)	10.49 ± 0.20	74 (92.5%)
11	81	47 (58.02%)	11.52 ± 0.21	73 (90.1%)	72	43 (59.72%)	11.60 ± 0.22	68 (94.4%)
12	86	45 (52.33%)	12.56 ± 0.19	83 (96.5%)	78	37 (47.44%)	12.55 ± 0.22	71 (91.0%)
13	89	48 (53.93%)	13.56 ± 0.19	81 (91.0%)	82	44 (53.66%)	13.59 ± 0.19	74 (90.2%)
14	74	39 (52.70%)	14.55 ± 0.20	65 (87.8%)	69	36 (52.17%)	14.59 ± 0.22	64 (92.8%)
15	98	57 (58.16%)	15.55 ± 0.21	92 (93.9%)	91	53 (58.24%)	15.59 ± 0.20	81 (89.0%)
16	77	40 (51.95%)	16.52 ± 0.23	69 (89.6%)	72	37 (51.39%)	16.46 ± 0.24	68 (94.4%)
17	94	53 (56.38%)	17.57 ± 0.20	89 (94.7%)	85	48 (56.47%)	17.56 ± 0.20	77 (90.6%)
18	76	44 (57.89%)	18.54 ± 0.17	70 (92.1%)	69	39 (56.52%)	18.49 ± 0.18	61 (88.4%)

Note: * Follow-up testing conducted after 6 months. Han ethnicity represents the majority ethnic group in China.

131

Supplementary Table S3. GAM/GAMM model fitting results

Measure	AIC	EDF	*F* value	P_{fdr} Value	Significant Change Period	Significant Age Range
Primary Site Baseline Sample						
Assessing interference inhibition via Stroop color-word task						
Stroop incongruent rt	1870.81	4.689	206.01	< 0.001	9.8 years (77.17%)	6.0 – 15.8 years
Stroop congruent rt	1810.29	5.545	190.55	< 0.001	7.4 years (58.27%)	6.0 – 13.4 years
Stroop neutral rt	1792.24	5.307	192.08	< 0.001	7.4 years (58.27%)	6.0 – 13.4 years
Stroop interference effect	2495.38	4.563	17.53	< 0.001	9.8 years (77.17%)	6.0 – 15.8 years
Assessing response inhibition via Go/No-Go task						
Go/No-Go d' value	1896.81	4.893	211.36	< 0.001	7.4 years (58.27%)	6.0 – 13.4 years
Go/No-Go Go acc	2068.47	4.504	84.43	< 0.001	6.0 years (47.24%)	6.0 – 12.0 years
Go/No-Go NoGo acc	1756.14	5.231	241.74	< 0.001	7.4 years (58.27%)	6.0 – 13.4 years
Go/No-Go Go rt	2168.91	4.770	141.00	< 0.001	7.7 years (60.63%)	6.0 – 13.7 years
Validation Site Baseline Sample						
Assessing interference inhibition via Stroop color-word task						
Stroop incongruent rt	1869.81	4.053	166.44	< 0.001	9.3 years (73.23%)	6.1 – 15.3 years
Stroop congruent rt	1892.26	5.318	123.59	< 0.001	7.3 years (57.48%)	6.1 – 13.3 years
Stroop neutral rt	1840.19	4.808	139.64	< 0.001	8.7 years (68.50%)	6.1 – 14.7 years
Stroop interference effect	2411.71	4.750	10.85	< 0.001	8.0 years (62.99%)	6.1 – 14.0 years
Assessing response inhibition via Go/No-Go task						
Go/No-Go d' value	2319.43	3.937	59.61	< 0.001	6.1 years (48.03%)	6.1 – 12.1 years
Go/No-Go Go acc	2396.53	2.991	11.36	< 0.001	3.4 years (26.77%)	7.5 – 10.9 years
Go/No-Go NoGo acc	2082.33	4.117	97.16	< 0.001	6.8 years (53.54%)	6.1 – 12.8 years
Go/No-Go Go rt	2105.27	3.961	113.50	< 0.001	8.1 years (63.78%)	6.1 – 14.1 years
Primary Site Test-Retest Sample (6-month interval)						
Assessing interference inhibition via Stroop color-word task						
Stroop incongruent rt	–170.30	6.655	128.88	< 0.001	9.7 years (76.38%)	6.4 – 16.1 years
Stroop congruent rt	199.86	6.775	152.90	< 0.001	8.3 years (65.35%)	6.2 – 14.5 years
Stroop neutral rt	95.49	6.773	159.88	< 0.001	7.8 years (61.42%)	6.2 – 14.0 years
Stroop interference effect	4166.97	4.986	8.89	< 0.001	9.7 years (76.38%)	6.2 – 15.9 years
Assessing response inhibition via Go/No-Go task						
Go/No-Go d' value	5367.18	6.217	47.69	< 0.001	6.1 years (48.03%)	6.5 – 12.6 years

Go/No-Go Go acc	4156.22	8.034	256.66	< 0.001	8.7 years (68.50%)	6.3 – 15.0 years
Go/No-Go NoGo acc	4859.79	7.509	122.50	< 0.001	7.9 years (62.20%)	6.2 – 14.1 years
Go/No-Go Go rt	4702.58	7.492	145.24	< 0.001	8.3 years (65.35%)	6.4 – 14.7 years

Note: AIC values for each model are used to compare goodness of fit, with lower AIC values indicating better model fit. EDF reflects the degree of nonlinearity in the smooth terms, with larger EDF values indicating more complex curves. *pfdr* values are -values adjusted for false discovery rate to correct for multiple comparisons. Significant change period indicates the duration of age ranges where corrected $p < 0.05$. **Abbreviations:** rt, reaction time; acc, accuracy.

Supplementary Table S4. Change rate analysis across developmental stages

Measure	Early Rapid Period (6–8 years)	Middle Sustained Period (9–12 years)	Late Developmental Period (13–15 years)	Stable Period (16–18 years)
Primary Site Baseline Sample (SD/year)				
Assessing interference inhibition via Stroop color-word task				
Stroop incongruent rt	0.451	0.230	0.109	N/A
Stroop congruent rt	0.591	0.223	0.085	N/A
Stroop neutral rt	0.537	0.233	0.094	N/A
Stroop interference effect	0.260	0.095	0.141	N/A
Assessing response inhibition via Go/No-Go task				
Go/No-Go d' value	0.369	0.314	0.097	N/A
Go/No-Go Go acc	0.310	0.207	N/A	N/A
Go/No-Go NoGo acc	0.422	0.311	0.098	N/A
Go/No-Go Go rt	0.371	0.239	0.155	N/A
Validation Site Baseline Sample (SD/year)				
Assessing interference inhibition via Stroop color-word task				
Stroop incongruent rt	0.367	0.232	0.099	N/A
Stroop congruent rt	0.604	0.191	0.073	N/A
Stroop neutral rt	0.466	0.220	0.079	N/A
Stroop interference effect	0.297	0.128	0.104	N/A
Assessing response inhibition via Go/No-Go task				
Go/No-Go d' value	0.261	0.209	N/A	N/A
Go/No-Go Go acc	0.123	0.095	N/A	N/A
Go/No-Go NoGo acc	0.315	0.233	N/A	N/A
Go/No-Go Go rt	0.287	0.198	0.156	N/A
Primary Site Test-Retest Sample (SD/6 months)				
Assessing interference inhibition via Stroop color-word task				
Stroop incongruent rt	0.672	0.480	0.252	0.022
Stroop congruent rt	0.977	0.563	0.079	N/A
Stroop neutral rt	0.964	0.512	0.198	N/A
Stroop interference effect	0.410	0.134	0.263	N/A
Assessing response inhibition via Go/No-Go task				
Go/No-Go d' value	0.738	0.281	N/A	N/A
Go/No-Go Go acc	1.060	0.517	0.099	N/A

Go/No-Go NoGo acc	0.893	0.352	0.358	N/A
Go/No-Go Go rt	0.762	0.455	0.201	N/A

Note ： N/A indicates no statistically significant change detected during this stage ($p > 0.05$, corrected with simultaneous confidence intervals). **Abbreviations:** rt, reaction time; acc, accuracy.

Supplementary Table S5. HDDM model diagnostic results

	Stroop Task		*Go/No-Go Task*		
Parameter	MCSE(M±SD)	R̂	MCSE(M±SD)	R̂	Converged
a	0.0002 ± 0.0001	1.0007	0.0003 ± 0.0002	1.0089	√
v	0.0008 ± 0.0006	1.0034	0.0007 ± 0.0005	1.0156	√
t	0.0002 ± 0.0001	1.0012	0.0004 ± 0.0002	1.0078	√
z	0.0001 ± 0.0001	1.0056	0.0002 ± 0.0001	1.0123	√

Note: MCSE = Monte Carlo Standard Error; R̂ = Potential Scale Reduction Factor (Gelman-Rubin statistic). While some R̂ values marginally exceed the conventional threshold of 1.01, all remain below 1.02. Additionally, effective sample sizes (bulk ESS) exceeded 400 for all parameters, indicating acceptable convergence according to current diagnostic recommendations (Pan et al., 2025). **Abbreviations**: ***a***, boundary separation; ***v***, drift rate; ***t***, non-decision time; ***z***, starting point bias.

Supplementary Table S6. Comparison of GAM model fit parameters controlling for HDDM parameters

Model	Nonlinearity Significance	R^2	ΔR^2	Relative Contribution (%)	AIC
Stroop incongruent reaction time (Interference inhibition)					
Baseline model	$p < 0.001$	0.522	/	/	3 139.58
Controlling ***v***	$p = 0.002$	0.394	–0.128	24.5	3 367.82
Controlling ***a***	p = 0.018	0.456	–0.066	12.6	3 241.73
Controlling ***t***	$p = 0.012$	0.468	–0.054	10.3	3 218.45
Controlling ***z***	$p < 0.001$	0.510	–0.012	2.3	3 156.92
Controlling all parameters	$p = 0.328$	0.312	–0.210	40.2	3 498.43
No-Go accuracy (Response inhibition)					
Baseline model	$p < 0.001$	0.648	/	/	3 308.68
Controlling ***z***	$p = 0.008$	0.524	–0.124	19.1	3 462.35
Controlling ***a***	$p = 0.025$	0.556	–0.092	14.2	3 398.74
Controlling ***t***	$p = 0.015$	0.578	–0.070	10.8	3 356.82
Controlling ***v***	$p = 0.003$	0.615	–0.033	5.1	3 341.26
Controlling all parameters	$p = 0.062$	0.418	–0.230	35.5	3 576.92

Note: ΔR^2 indicates the change in R^2 relative to the baseline model; "Nonlinearity Significance" refers to whether the age smooth term remains significant after controlling for the specified HDDM parameter. **Abbreviations**: ***a***, boundary separation; ***v***, drift rate; ***t***, non-decision time; ***z***, starting point bias.

Supplementary Figures

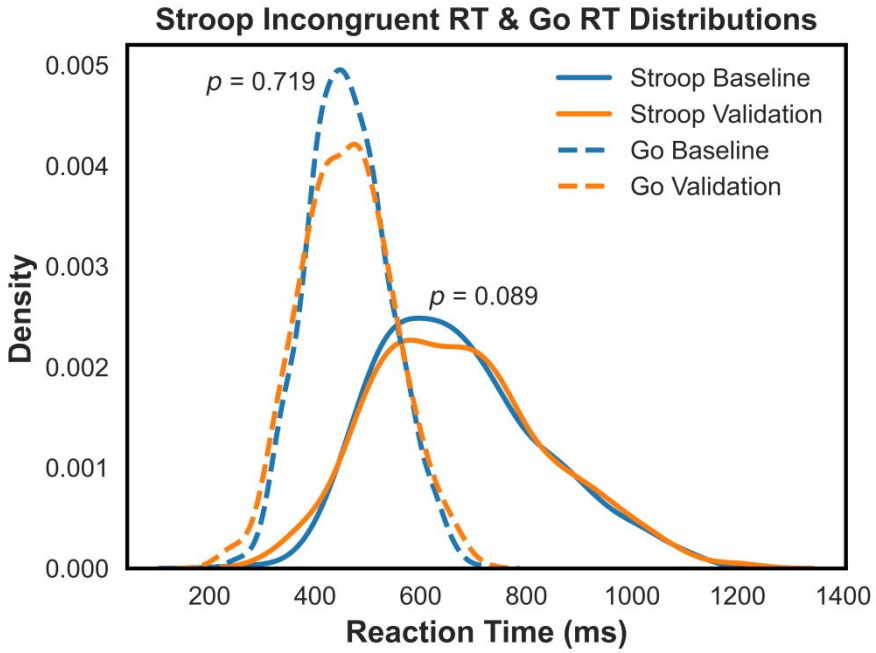

Supplementary Figure S1. Comparison of sample distributions between primary site and cross-site data

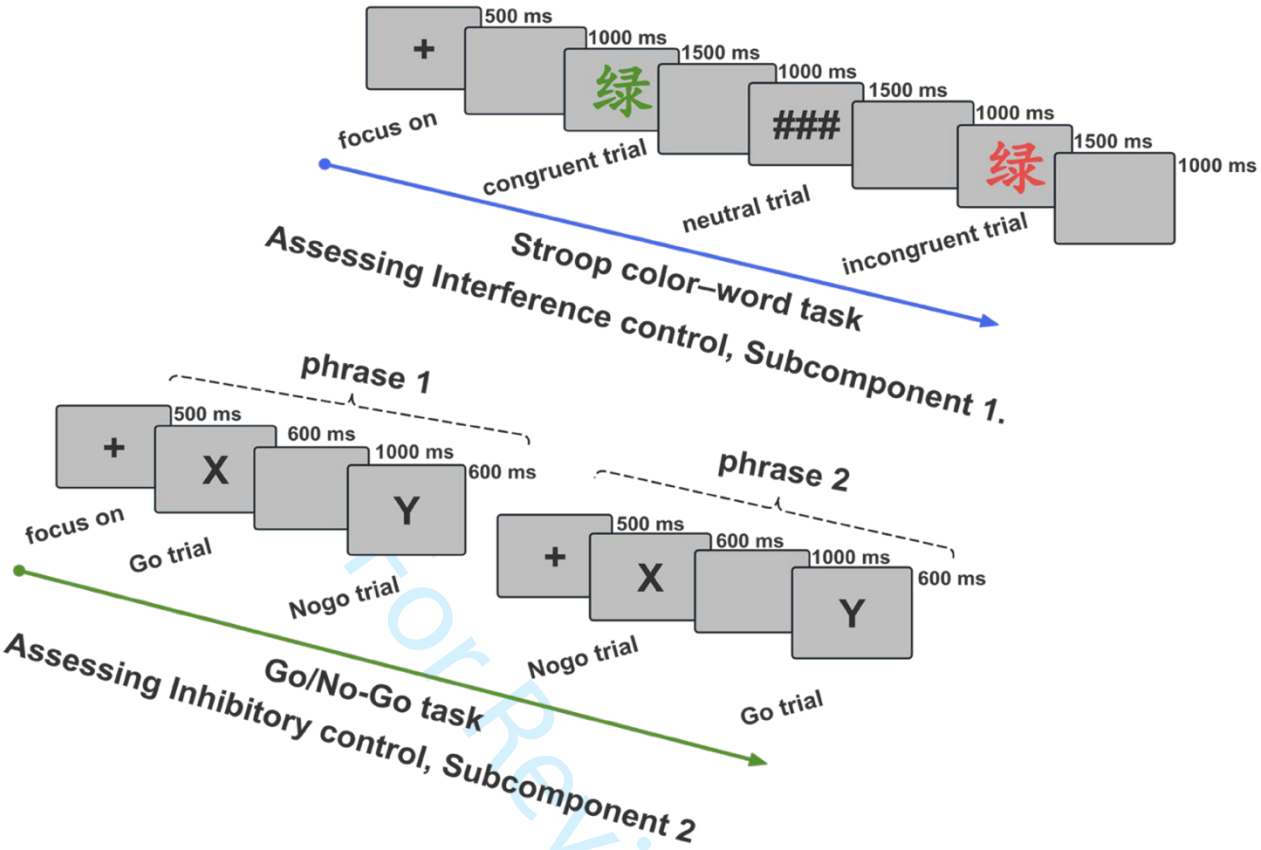

Supplementary Figure S2. Schematic illustration of the Stroop color-word task and Go/No-Go task paradigms.

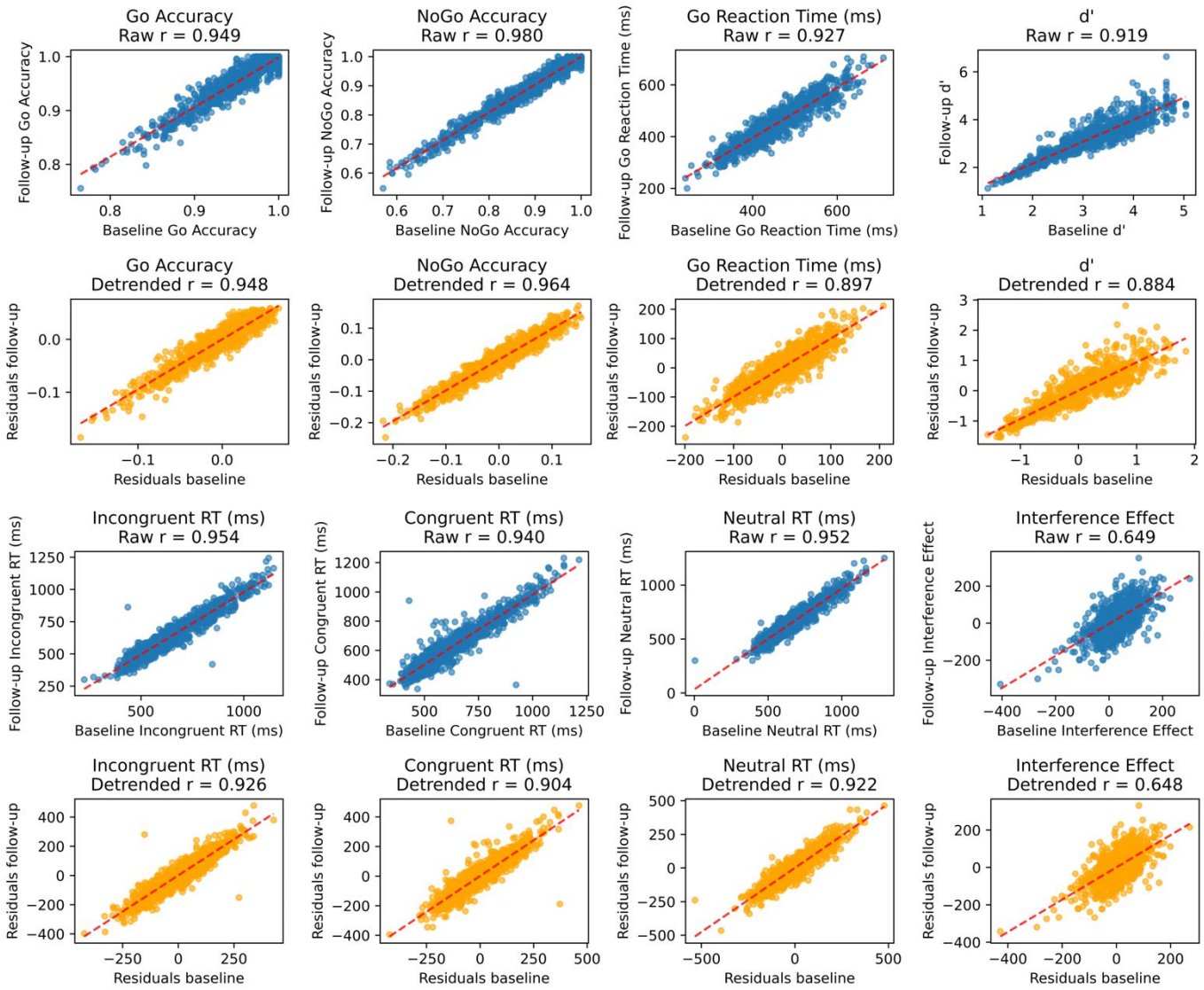

147 **Supplementary Figure S3. Stability analysis results for test-retest reliability**

148 **measurements**

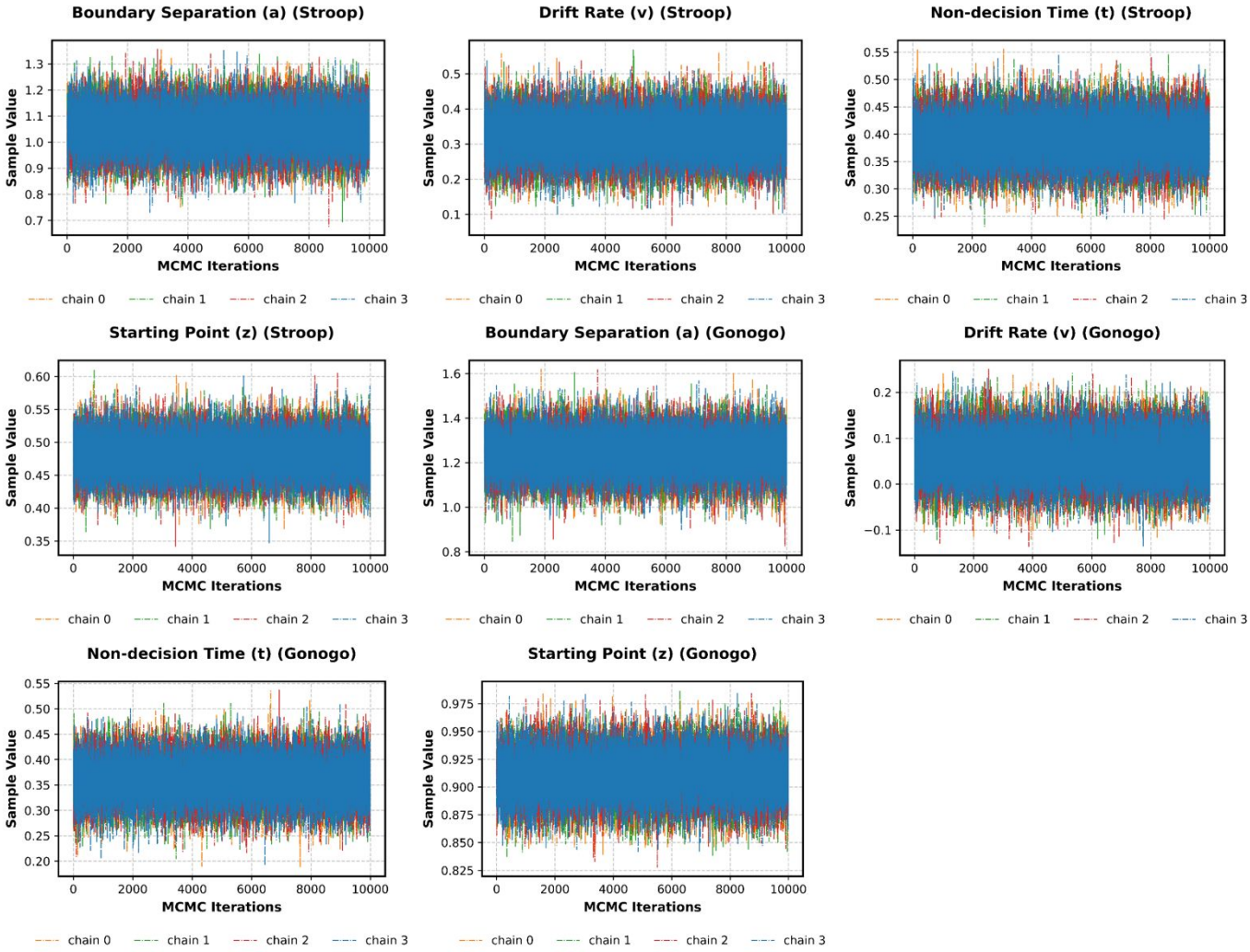

149 **Supplementary Figure S4. HDDM model diagnostic results trace**

150 **Note:** The convergence and reliability of MCMC chains are demonstrated by stable oscillations around

151 constant values with overlapping trajectories across different chains, producing a characteristic "caterpillar"

152 pattern. **Abbreviations**: MCMC = Markov Chain Monte Carlo; ***a***, boundary separation; ***v***, drift rate; ***t***, non-

153 decision time; ***z***, starting point bias.

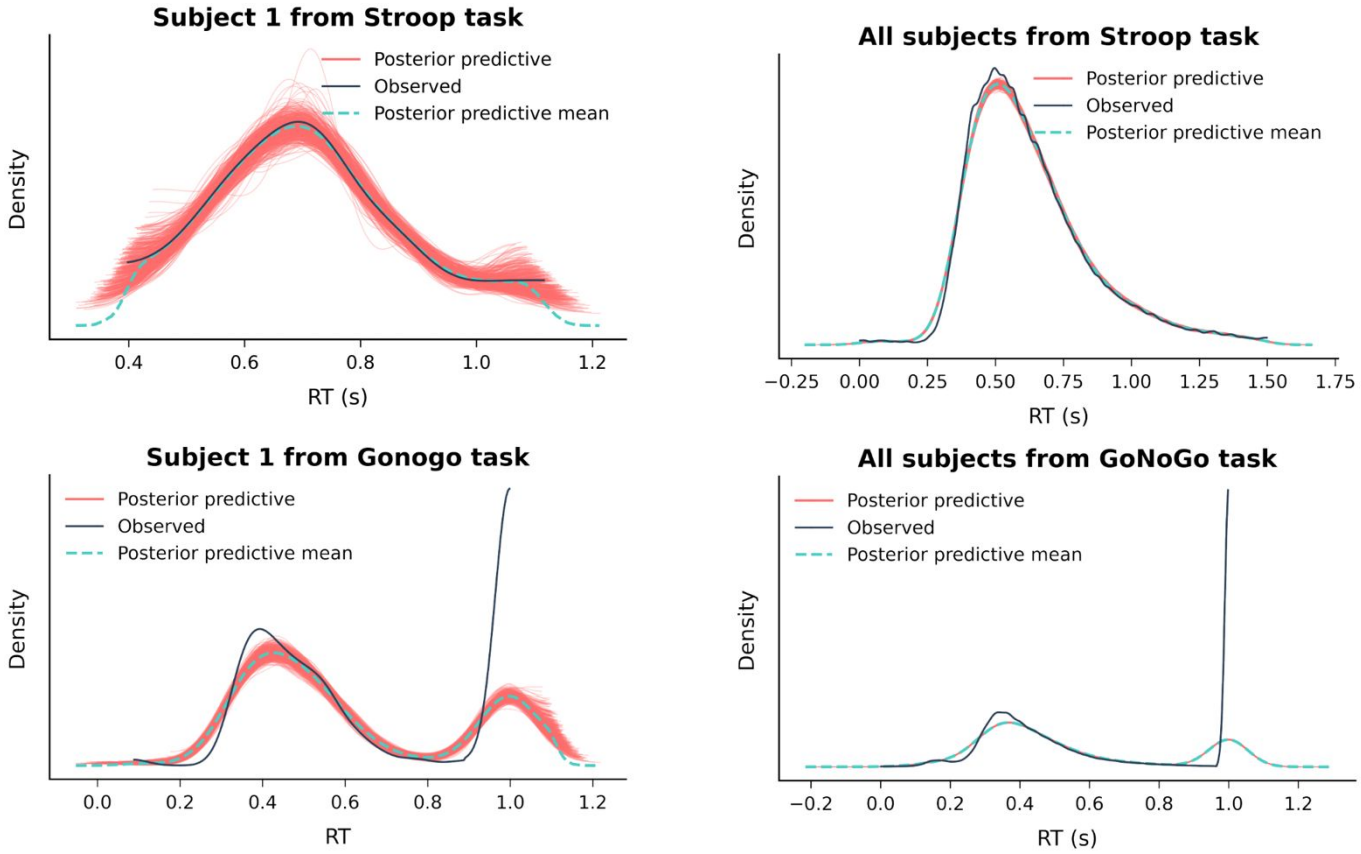

Supplementary Figure S5. HDDM posterior predictive check results

Note: Posterior predictive check plots comparing observed and model-predicted reaction time (RT) distributions at individual and group levels. Black lines represent observed RT distributions. Pink lines indicate individual posterior predictive samples, with each line representing a predicted RT distribution derived from a single posterior sample. Blue dashed lines show the mean predicted RT distribution averaged across all posterior predictive samples.

Supplementary References

Akiba, T., Sano, S., Yanase, T., Ohta, T., & Koyama, M. (2019). Optuna: A next-generation hyperp. *Proceedings of the 25th ACM SIGKDD International Conference on Knowledge Discovery & Data Mining*, 2623–2631. https://doi.org/10.1145/3292500.3330701

Ambrosi, S., Śmigasiewicz, K., Burle, B., & Blaye, A. (2020). The dynamics of interference control across childhood and adolescence: Distribution analyses in three conflict tasks and ten age groups. *Developmental Psychology*, *56*(12), 2262–2280. https://doi.org/10.1037/dev0001122

Dienes, Z. (2016). How Bayes factors change scientific practice. *Journal of Mathematical Psychology*, *72*, 78–89. https://doi.org/10.1016/j.jmp.2015.10.003

Gorka, A. X., Philips, R. T., Torrisi, S., Claudino, L., Foray, K., Grillon, C., & Ernst, M. (2023). The Posterior Cingulate Cortex Reflects the Impact of Anxiety on Drift Rates During Cognitive Processing. *Biological Psychiatry: Cognitive Neuroscience and Neuroimaging*, *8*(4), 445–451. https://doi.org/10.1016/j.bpsc.2022.03.010

Habets, P. C., Thomas, R. M., Milaneschi, Y., Jansen, R., Pool, R., Peyrot, W. J., Penninx, B. W. J. H., Meijer, O. C., van Wingen, G. A., & Vinkers, C. H. (2023). Multimodal Data Integration Advances Longitudinal Prediction of the Naturalistic Course of Depression and Reveals a Multimodal Signature of Remission During 2-Year Follow-up. *Biological Psychiatry*. https://doi.org/10.1016/j.biopsych.2023.05.024

Kruschke, J. K., & Liddell, T. M. (2018). The Bayesian New Statistics: Hypothesis testing, estimation, meta-analysis, and power analysis from a Bayesian perspective. *Psychonomic Bulletin & Review*, *25*(1), 178–206. https://doi.org/10.3758/s13423-016-1221-4

Letkiewicz, A. M., Wakschlag, L. S., Briggs-Gowan, M. J., Cochran, A. L., Wang, L., Norton, E. S., & Shankman, S. A. (2024). Preadolescent externalizing and internalizing symptoms are differentially related to drift-diffusion model parameters and neural activation during

a go/no-go task. *Journal of Psychiatric Research*, *178*, 405–413. https://doi.org/10.1016/j.jpsychires.2024.08.038

Pan, W., Geng, H., Zhang, L., Fengler, A., Frank, M. J., Zhang, R.-Y., & Chuan-Peng, H. (2025). dockerHDDM: A User-Friendly Environment for Bayesian Hierarchical Drift-Diffusion Modeling. *Advances in Methods and Practices in Psychological Science*. https://doi.org/doi.org/10.1177/2515245924129

Ratcliff, R., Huang-Pollock, C., & McKoon, G. (2018). Modeling individual differences in the go/no-go task with a diffusion model. *Decision*, *5*(1), 42. https://doi.org/10.1037/dec0000065

Ratcliff, R., Smith, P. L., Brown, S. D., & McKoon, G. (2016). Diffusion Decision Model: Current Issues and History. *Trends in Cognitive Sciences*, *20*(4), 260–281. https://doi.org/10.1016/j.tics.2016.01.007

Schultebraucks, K., Ben-Zion, Z., Admon, R., Keynan, J. N., Liberzon, I., Hendler, T., & Shalev, A. Y. (2022). Assessment of early neurocognitive functioning increases the accuracy of predicting chronic PTSD risk. *Molecular Psychiatry*, *27*(4), Article 4. https://doi.org/10.1038/s41380-022-01445-6

Szul, M. J., Bompas, A., Sumner, P., & Zhang, J. (2020). The validity and consistency of continuous joystick response in perceptual decision-making. *Behavior Research Methods*, *52*(2), 681–693. https://doi.org/10.3758/s13428-019-01269-3

Webb, C. A., Cohen, Z. D., Beard, C., Forgeard, M., Peckham, A. D., & Björgvinsson, T. (2020). Personalized prognostic prediction of treatment outcome for depressed patients in a naturalistic psychiatric hospital setting: A comparison of machine learning approaches. *Journal of Consulting and Clinical Psychology*, *88*(1), 25–38. https://doi.org/10.1037/ccp0000451

210 Yang, H., & van Vugt, M. (2025). “Sticky” thinking disrupts decision making for individuals
211 with a tendency toward worry and depression. *Emotion*, *25*(4), 997–1010.
212 https://doi.org/10.1037/emo0001449
213